Lin, J.-Y., Wang, H., Oh, W. D., Lee, J., Kwon, E., You, S., Lin, C.-H. and Lin, K.-Y. A. (2021) Integrated MOF-mesh and TEMPO-grafted carbon fiber as a sandwich-like catalytic system for selective valorization of lignin-derived compound under microwave irradiation. *Chemical Engineering Journal*, 411, 128605.

(doi: 10.1016/j.cej.2021.128605)

This is the Author Accepted Manuscript.

There may be differences between this version and the published version. You are advised to consult the publisher's version if you wish to cite from it.

https://eprints.gla.ac.uk/229091/

Deposited on: 21 January 2021

Enlighten – Research publications by members of the University of Glasgow
http://eprints.gla.ac.uk

Manuscript Click here to view linked References

Integrated MOF-mesh and TEMPO-grafted Carbon Fiber as a Sandwich-like Catalytic System for Selective Valorization of Lignin-derived Compound under Microwave Irradiation

Jia-Yin Lin[a], *Haitao Wang*[b], *Wen Da Oh*[c], *Jechan Lee*[d], *Eilhann Kwon*[e], *Siming You*[f], *Chia-Hua Lin*[g,*], *and Kun-Yi Andrew Lin*[a,*]

[a]Department of Environmental Engineering & Innovation and Development Center of Sustainable Agriculture & Research Center of Sustainable Energy and Nanotechnology, National Chung Hsing University, 250 Kuo-Kuang Road, Taichung, Taiwan

[b]Key Laboratory of Pollution Processes and Environmental Criteria, College of Environmental Science and Engineering, *Nankai University*, Tianjin 300071, P. R. China

[c]School of Chemical Sciences, Universiti Sains Malaysia, 11800 Penang, Malaysia

[d]Department of Environmental and Safety Engineering, *Ajou University*, Suwon 16499, Republic of Korea

[e]Department of Environment and Energy, Sejong University, 209 Neungdong-ro, Gunja-dong, Gwangjin-gu, Seoul, Republic of Korea

[f]James Watt School of Engineering, University of Glasgow, Glasgow G12 8QQ, UK

[g]Department of Biotechnology, National Formosa University, Yunlin 63208, Taiwan

*Corresponding Authors. E-mail address: linky@nchu.edu.tw (K.-Y. A. Lin); sptong@zjut.edu.cn (Shaoping Tong)

Abstract

Oxidation of vanillyl alcohol to vanillin represents a critical step towards sustainable valorization of lignocellulosic biomass. Although catalytic oxidation of vanillyl alcohol by Cu and 2,2,6,6-tetramethylpiperidine 1-oxyl (TEMPO) is promising for vanillyl alcohol oxidation, the traditional Cu/TEMPO adopts homogeneous Cu ions and TEMPO, which are difficult for recovery and reuse. In this study, a unique sandwich-like catalytic system (SCS), which comprises HKUST-1 mesh and TEMPO-grafted on carbon cloth, is developed as a heterogeneous catalyst for vanillyl alcohol oxidation. Through the electro-chemical technique, copper (Cu) mesh is used as a source of Cu to grow HKUST-1 directly, whereas carbon cloth is functionalized by TEMPO via covalent bonds. These resultant materials are then stacked to achieve layer-by-layer contacts between HKUST-1 and TEMPO, and enable flow-through reactions of VAL oxidation. Especially, such a SCS exhibits much higher conversion of vanillyl alcohol to vanillin under microwave irradiation than conventional oven heating. SCS could achieve 100% of conversion, 100% of selectivity and 100% of yield of vanillin at 120 °C for 60 min. This full conversion of vanillyl alcohol to vanillin surpasses almost all the reported values by other processes in literature, and SCS could be also reusable and continuously implemented for vanillyl alcohol conversion to vanillin. The used HKUST-1 mesh could retain crystalline structures of HKUST-1, whereas TEMPO is also preserved on TEMPO@CC, indicating that SCS would be a stable and reusable integrated catalyst for vanillyl alcohol oxidation to vanillin.

Keywords: hybrid mesh, MOFs, HKUST-1, carbon cloth, lignin, vanillyl alcohol, vanillin

1. Introduction

Lignocellulosic biomass and biowaste are considered as a renewable resource which can be further utilized and valorized [1, 2]. Many approaches have been proposed for valorizing lignocellulosic biomass, such as pyrolysis and oxidation [3-8]. Although pyrolysis can rapidly decompose biomass to several products, chars from pyrolysis remain as a challenging issue and many other issues still exist at large-scale operations [9, 10]. In contrast, oxidation of lignocellulosic biomass seems a more feasible and favorable approach as oxidation processes are milder and more environmentally benign [6, 11-15]. More importantly, oxidation of lignin-derived molecules can generate many valuable compounds with versatile functions [10].

As lignin contains relatively complex structures, oxidation processes are usually investigated by oxidizing lignin-derived model compounds [2, 5, 6, 16-19]. As the β-O-4 has been regarded as the most typical sub-structure of lignin [20], decomposition of these β-O-4 sub-structures of lignin produces several low-molecular-weight derivatives. Among these lignin-derived molecules, such as 3-methoxy-4-hydroxycinnamic acid [21-25], and vanillyl alcohol (VAL) [16, 26-28], VAL is particularly attractive as oxidation of VAL can produce a high-value-added compound, vanillin (VN), which is a widely-consumed flavorant used in foods, perfumes, cosmetics, pharmaceuticals and drinks [16]. Conventionally, vanillin is extracted from *Vanilla planifolia*; however chemical synthesis of vanillin has become a dominant source because of vast demand of vanillin. To date, one of the most popular route for synthesizing vanillin requires usage of petrochemical raw chemical, guaiacol, through multiple steps [29]. Recently, biological production of vanillin has been also proposed by using bacteria (e.g., *Rhodococcus jostii* RHA1) through decomposition of lignin into vanillin [30, 31] and fermentation of ferulic acid [32, 33].

Even though a few studies have converted VAL to VN via oxidation, these researches employed un-recyclable oxidant, H_2O_2, [34-36] and a large amount of H_2O_2 is required because of stoichiometric chemistry. More importantly, these H_2O_2-based oxidation methods usually lead to very low conversion of VAL (C_{VAL}), selectivity for VN (S_{VN}) and yield of VN (S_{VN}) [6, 18, 37, 38].

Since recent interests of oxidative reactions are focused on utilization of oxygen gas molecules (O_2) as a direct oxidant [39-41], it would be certainly sustainable to develop a process of VAL conversion by using O_2 to oxidize VAL to VN. To this end, an useful oxidation process of utilizing O_2, especially for oxidation of alcohols, is revealed by using Cu as a metal catalyst and 2,2,6,6-tetramethylpiperidine 1-oxyl (TEMPO) as an organic oxidation co-catalyst together with O_2 as an oxidant [42]. The integration of Cu/TEMPO has been validated as an effective catalytic system for oxidizing alcohols to corresponding aldehydes [39-41, 43, 44]. As VAL is an alcohol, which can be further oxidized to produce an aldehyde group, forming VN, The integration of Cu/TEMPO would be useful for VAL oxidation.

Nevertheless, the traditional integration of Cu/TEMPO uses homogeneous Cu ions and TEMPO [45] but recovering Cu ion and TEMPO from reactions is certainly highly-challenging. To address the aforementioned issue, it would be critical to develop heterogeneous catalysts containing Cu and TEMPO moieties. Moreover, these heterogeneous catalysts must be easily implemented, recovered and reused. Even though powders and particles (or nanoparticles) are promising catalysts, fine powders/particles are actually still difficult to recover and reuse. Thus, macroscale substrate-supported catalysts, on which nanoscale active components or molecular compounds are deposited, would be advantageous because marco-substrates allow them to be easily operated and nanoscale active components would provide high

activities. Among various types of macroscale substrates, mesh-like substrates would be highly favorable as they can be grafted with nanoscale components but still allow reactants to flow-through these mesh-like substrates for target reactions. To this end, the present study proposes to develop mesh-supported catalysts containing Cu and TEMPO. In the case of Cu-containing mesh, while Cu mesh is readily available, Cu mesh exhibits very low surface areas and active sites. Therefore, Cu-based metal organic frameworks (MOFs) is then particularly fabricated by direct growth of Cu-MOFs (i.e., HKUST-1) on Cu mesh, which not only acts as a support but also serves as a Cu source to grow HKUST-1. On the other hand, TEMPO would be grafted on a stable and robust mesh-like substrate, carbon cloth (CC), via covalent bonds. The resultant HKUST-1 mesh and TEMPO@CC would be inter-stacked to form a sandwich-like catalytic system (SCS) for allowing layer-by-layer contacts between Cu and TEMPO. Once reactants (i.e., VAL) flow through this SCS, VAL would react with Cu and then TEMPO continuously to transform into VN.

Moreover, as such a reaction of VAL oxidation is a solvothermal reaction, heating processes have been a key to conversion efficiencies. In this study, conventional oven heating (COH) and microwave irradiation (COH) have been also adopted and compared for VAL conversion by SCS. To our best knowledge, such a SCS or hybrid-mesh catalysts have been never reported for VAL conversion and thus fabrication techniques and corresponding catalytic behaviors given here would be highly useful and insightful.

2. Experimental

2.1 Materials

All chemicals employed in this study were of analytical-regent grade and were used without further purification. Cu mesh (100 mesh, 99.9% copper) was purchased from

May Chun Company Limited (Taiwan). Carbon cloth (CC) was provided by Taicarbon Company (Taiwan). Copper (II) nitrate trihydrate (Cu $(NO_3)_2 \cdot 3H_2O$) and iso-propanol (IPA) were obtained from Union Chemicals (Taiwan), whereas benzene-1,3,5-tricarboxylic acid (H_3BTC) was purchased from Showa Chemical Co. Ltd (Taiwan), and 4-Hydroxy-TEMPO was received from Merck (Germany). Tetrahydrofuran and N,N'-dicyclohexylcarbodiimide were purchased from Sigma-Aldrich (USA).

2.2 Preparation of HKUST-1 MESH

A piece of Cu mesh (0.5 cm × 1 cm) with a thickness of 0.1mm was immersed in 3M HCl and placed in an ultrasound bath for 15 min to remove its surficial impurities followed by rinsing it with DI water and ethanol. Next, Cu mesh was used as anode, whereas titanium plate (99.9% Titanium) was used as the cathode. A mixture of ethanol and DI water (1:1) was then employed as the electrolyte to which 100 mg H_3BTC was directly added. Subsequently, the anodizing growth of HKUST-1 mesh was carried out at 5V for 20 min at room temperature as illustrated in Fig. 1(a). The resultant HKUST-1 mesh was then rinsed with ethanol and DI water thoroughly and dried at 80 °C in oven for 12h to afford HKUST-1 mesh.

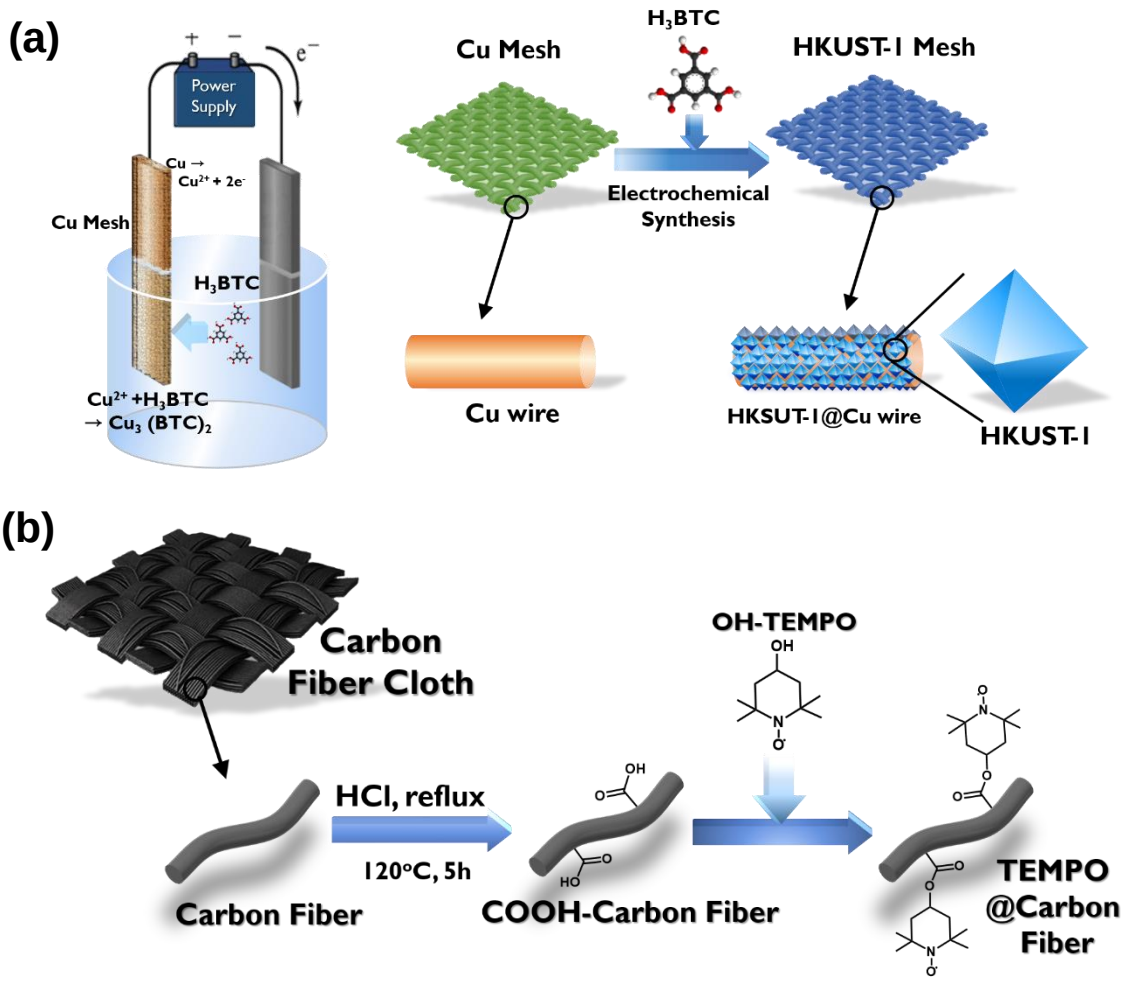

Figure 1. Schematic illustrations for preparation of (a) HKUST-1 mesh via the one-step electrochemical synthesis and (b) TEMPO@CC

2.3 Synthesis of TEMPO@CC

The synthetic route for TEMPO@CC could be illustrated in Fig. 1(b). Firstly, a piece of CC (0.5 cm × 1 cm) was added in a flask with 50 mL of HCl and 100 mL of DI water. Then, the mixture flask with a condenser was placed on a temperature-controllable stirring plate. The resulting mixture was refluxed for 5h under 110oC. After cooling temperature to 40 °C, the acid-treated carbon cloth was washed with DI water repeatedly and dried in oven at 80 °C overnight. This resultant carboxyl-functionalized CC, together with OH-TEMPO (0.4 g) and N,N'-dicyclohexylcarbodiimide (0.578 g)

were then mixed in 20 mL of tetrahydrofuran at ambient temperature for 72 hours. Finally, the TEMPO-grafted CC (i.e., TEMPO@CC) was washed with methanol/DI water and then dried at 80oC in oven overnight. Electron spin resonance (ESR) spectrum of TEMPO@CC was implemented by a Bruker EMX Plus X-Band spectrometer.

2.4 Conversion of VAL to VN

Catalytic conversion of VAL was implemented in a cylindrical Teflon-lined reactor in which the bundled sandwich-like catalyst (two HKUST-1 meshes inter-stacked with two TEMPO@CC) was hanged and suspended in the center of the reactor to allow reactants to flow through. In a typical experiment, 10 mg of VAL and 20 mL of iso-propanol were added to the Teflon-lined reactor. Next, the mixture was then heated by MWI or in a conventional oven to start VAL conversion. The MWI system was Ethos UP (Milestone, Italy) whose volume was 70 liters with two 950 watt magnetrons and its temperature range is from the ambient temperature to 220 °C. The conventional oven used in this study was Memmert (Germany), ULE 400, whose volume was 53 liters and temperature range is from 30 to 220 °C with natural convection. After pre-set reaction times, sample aliquots were withdrawn from the vessel and filtrated through syringe membrane disks (0.22 μm, PVDF). The filtrates were analyzed for concentrations of reactant and products using a HPLC (Kanuer Azura, Germany) with a UV-Vis detector (275 nm) and a reverse-phase C-18 column. The mobile phase consisted of aqueous acetonitrile (20%), acetic acid (1%) and distilled water (79%) at a flowrate of 1.0 mL/min.

Based on previous literatures [4, 34], chemical oxidation of VAL to VN was quantified as follows:

$$\text{Conversion of VAL } (C_{VAL}) = \frac{\text{Consumed VAL}}{\text{Total VAL}} \times 100\% \quad (1)$$

$$\text{Selectivity for VN } (S_{VN}) = \frac{\text{VN (mol)}}{\text{Consumed VAL (mol)}} \times 100\% \quad (2)$$

$$\text{Yield } (Y_{VN}) = \frac{\text{VN (mol)}}{\text{Total VAL (mol)}} \times 100\% \quad (3)$$

3. Results and discussion

3.1 Characterization of HKUST-1 mesh and TEMPO@CC

To characterize HKUST-1 mesh, the picture of pristine Cu mesh was firstly revealed in Fig. 2(a) and it exhibited the very typical reddish brown color. Fig. 2(b) and (c) further show that the pristine Cu mesh was extremely smooth. After the anodic growth of HKUST-1 on the Cu mesh, the color of the mesh had completely changed from reddish brown to blue as seen in Fig. 2(a). Another noteworthy feature was that the blue color was very homogeneous all over the entire piece, suggesting that the electro-chemical technique was certainly capable of growing HKUST-1 on the mesh. Closer views (Fig. 2(d) and (e)) further reveal that the originally smooth surface of mesh had been modified, and fully and uniformly covered by octahedral crystals. This octahedral morphology was consistent to the typical morphology of HKUST-1, suggesting that HKUST-1 was successfully grown on the Cu mesh.

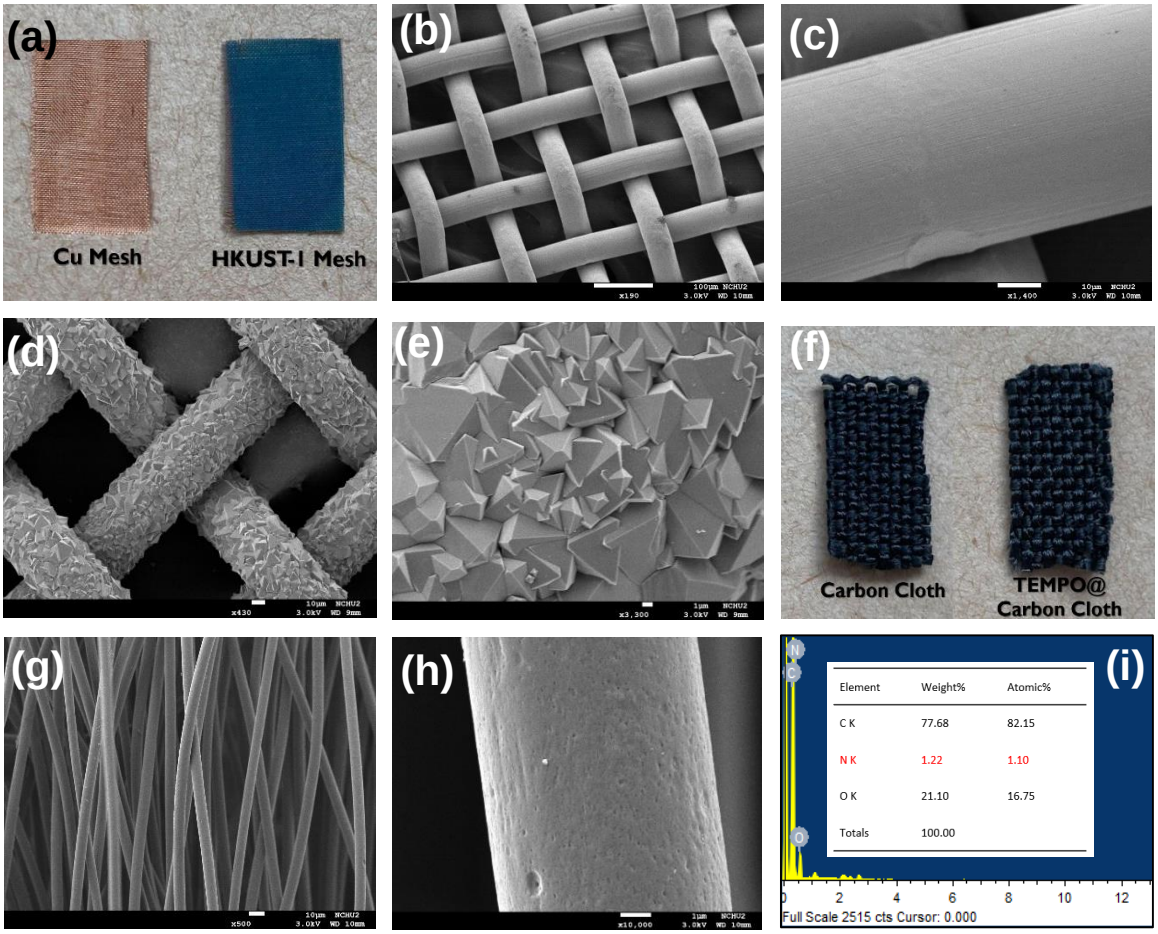

Fig. 2. (a) Pictures of Cu mesh and HKUST-1 mesh; SEM images of (b), (c) pristine Cu mesh; (d), (e) HKUST-1 mesh; (f) pictures of carbon cloth and TEMPO@CC; (g),(h) SEM image of TEMPO@CC; and (i) EDS analysis of TEMPO@CC.

Fig. 3(a)-(d) further display the elemental mapping result of this HKUST-1 mesh and elements of C, O and Cu were easily detected and evenly distributed all over the mesh, demonstrating that the Cu mesh had been completely and homogeneously covered by HKUST-1. Fig. 4(a) also confirms that after the anodizing Cu mesh with H_3BTC, the XRD pattern of Cu mesh had changed significantly to exhibit a series of peaks ranging from 5 to 45 °, which were in line with the signature peaks of HKUST-1, validating that HKUST-1 was certainly and successfully grown on the mesh.

On the other hand, pictures of CC and the TEMPO-grafted CC were displayed in

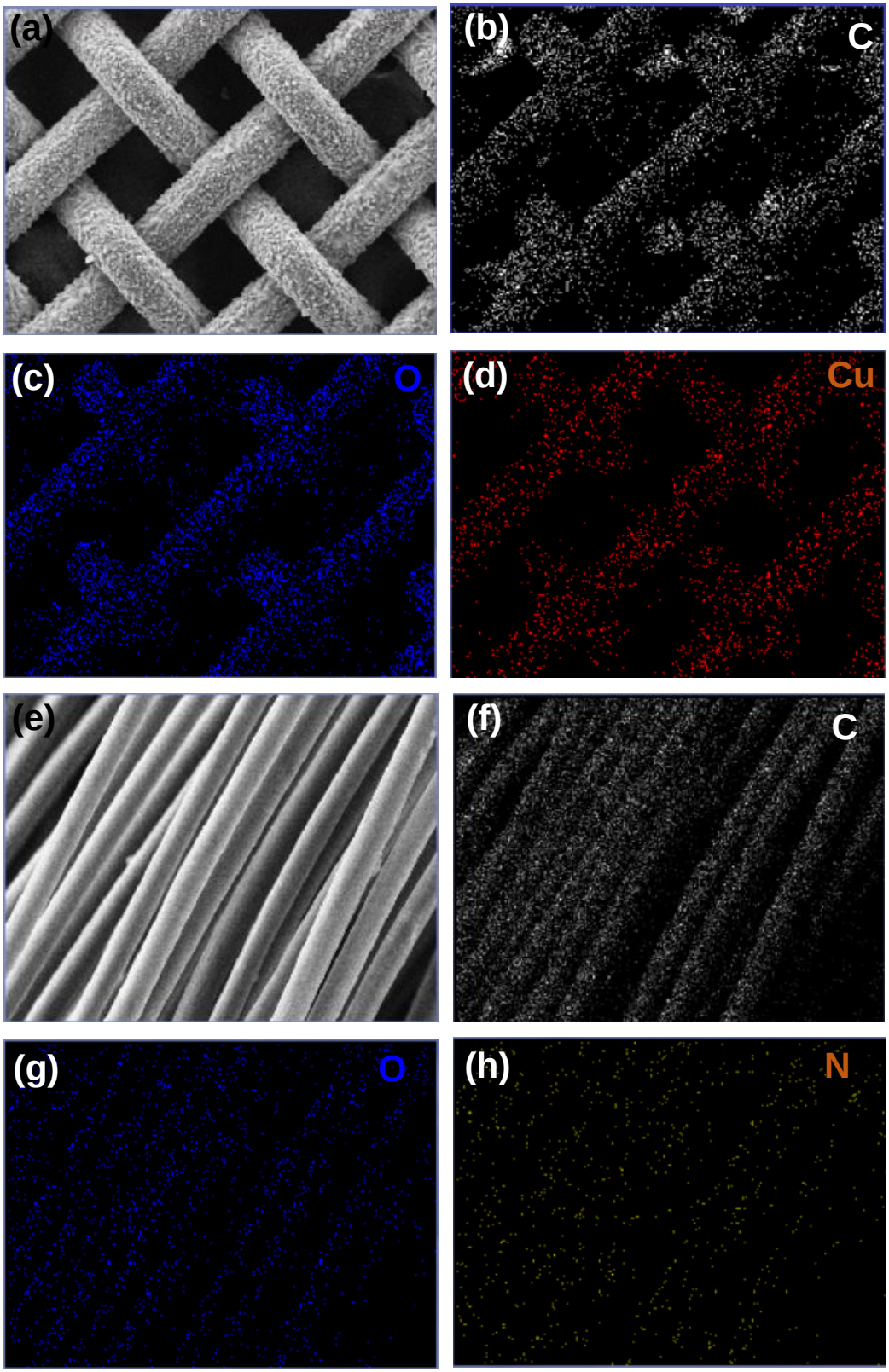

Fig. 3 Elemental mapping analysis: (a) Image of the selected area, (b) carbon, (c) oxygen and (d) nitrogen of HKUST-1 mesh; (e) image of the selected area, (f) carbon, (g) oxygen and (h) nitrogen of TEMPO@CC.

Fig. 2(f), and no huge differences between the pristine CC and TEMPO@CC were observed. Closer views of TEMPO@CC (Fig. 2(g),(h)) confirmed that fibrous configuration of carbon fibers in CC was well-retained and no obvious damage or destruction was noted. Nevertheless, Fig. 2(i) reveals that elements of N and O were detected, suggesting that CC had been modified and functionalized. Fig. 3(e)-(h) also display that elements of O and N were homogeneously distributed all over these fibers, suggesting that the surficial modification and functionalization on carbon fibers was uniformly-implemented.

Moreover, IR spectra of CC and TEMPO@CC were displayed in Fig. 4(b). While CC exhibited relatively limited IR peaks, TEMPO@CC showed several noticeable peaks in the range of 1000~1700 cm^{-1} and 2800~3000 cm^{-1}. In comparison to the IR spectrum of OH-TEMPO, these noticeable peaks of TEMPO@CC could be attributed to TEMPO. Specifically, the peaks at 875, 1580, 1620 cm^{-1} would be ascribed to C-H bonds derived from tetramethyl groups of TEMPO [46]. Additionally, the peak at 2944 cm^{-1} could be assigned to CH_3 bonds in TEMPO [46]. The presence of these peaks suggested that TEMPO was grafted onto CC. More importantly, as TEMPO is a strong radical, ESR analysis was then employed to determine TEMPO@CC (Fig. 4(c)). Even though no signal was observed in the case of CC, a typical three-line pattern with equal intensities [47, 48], which was attributed to TEMPO radicals [47, 48], could be easily measured. These characterizations all indicated that TEMPO was grafted onto CC.

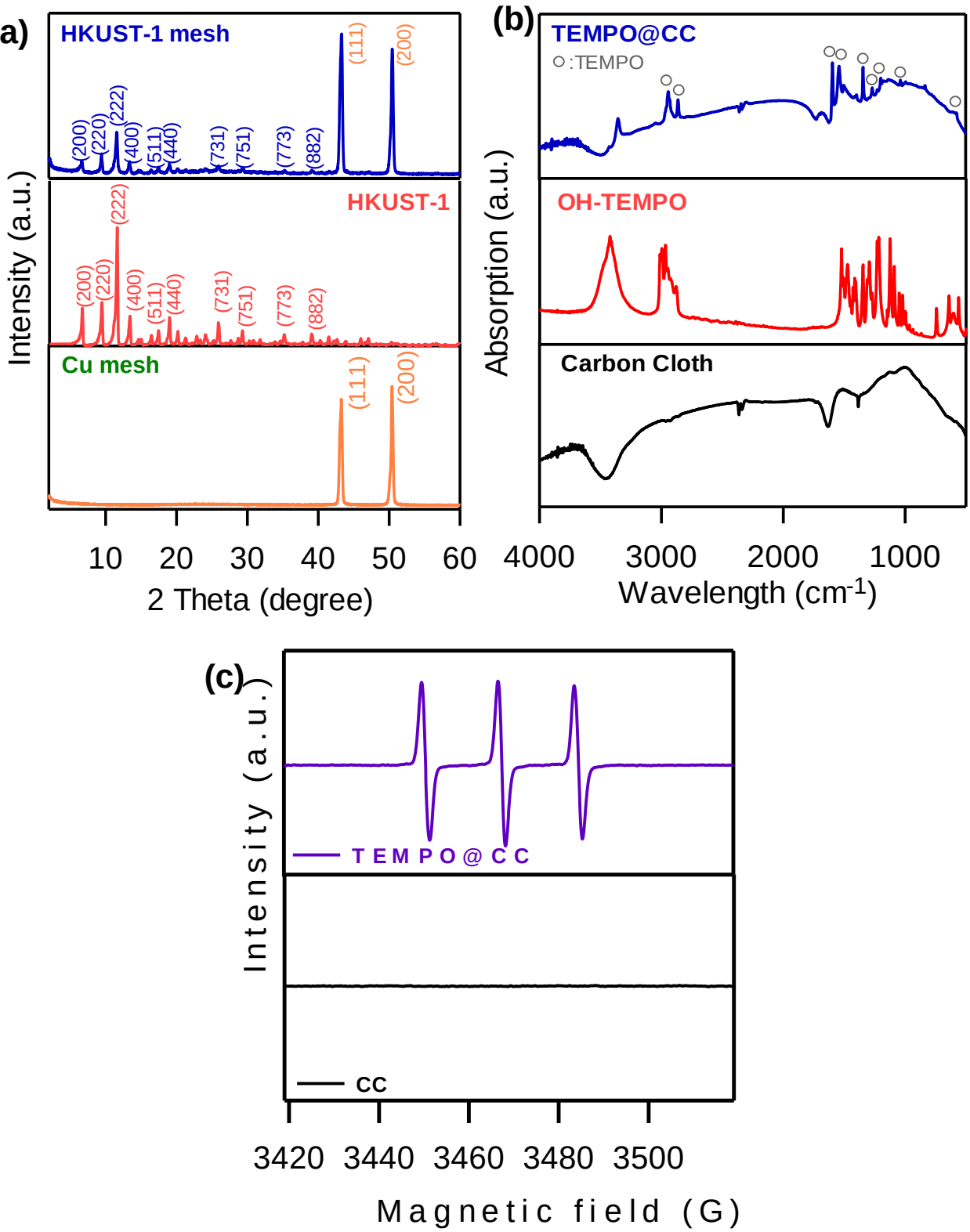

Fig. 4 (a) XRD patterns of HKUST-1 mesh, HKUST-1, and Cu mesh, (b) IR spectra of TEMPO@CC, CC, and TEMPO; and (c) ESR analyses of TEMPO@CC and CC.

As the Cu mesh and CC had been modified and deposited with HKUST-1 and TEMPO moieties, respectively, their textural properties might be also changed. Thus, their N_2 sorption isotherms were then measured. Fig. 5(a) shows N_2 sorption isotherms of pristine Cu mesh and HKUST-1 mesh. Since the pristine Cu mesh exhibited very smooth surface, its N_2 sorption capacity was extremely low, leading to a very low surface area of 10 m^2/g.

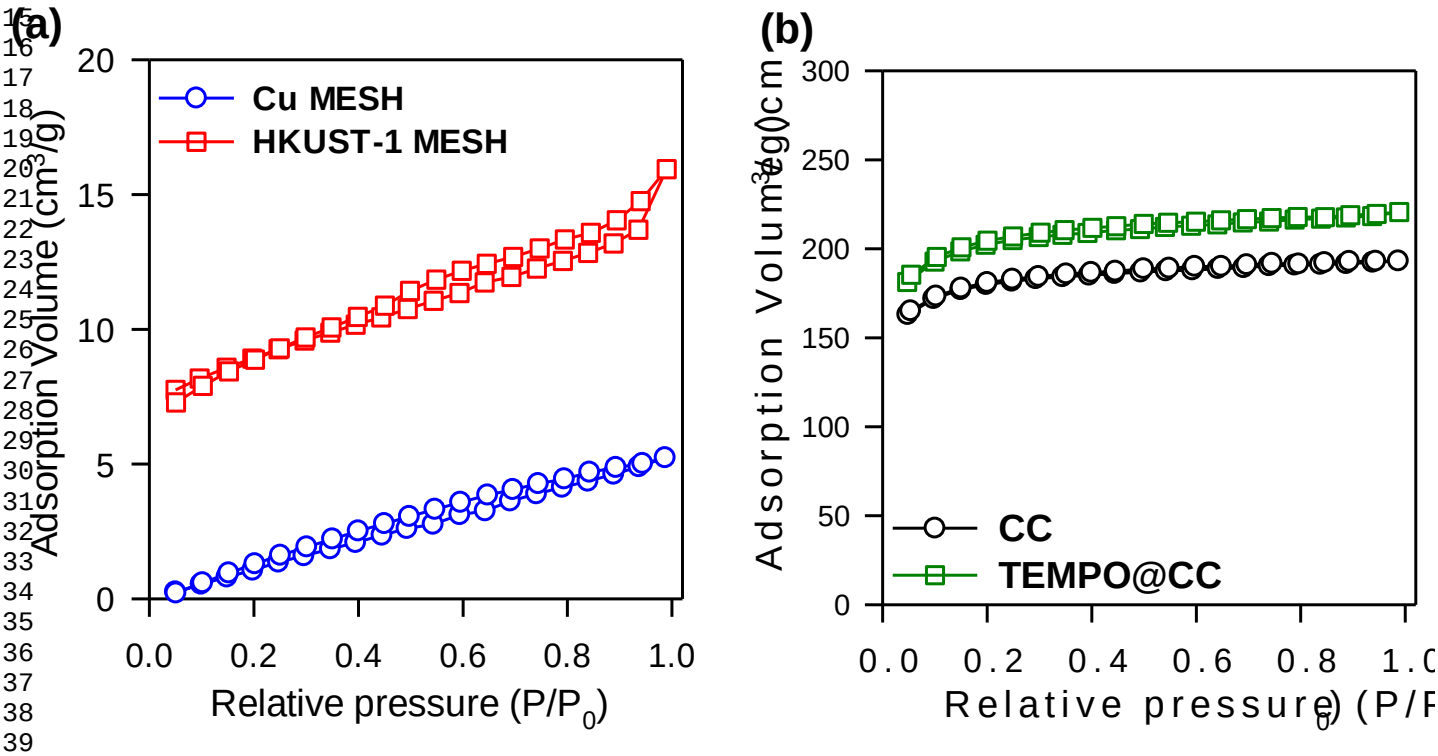

Fig. 5 N_2 sorption isotherms of (a) Cu mesh and HKUST-1 mesh; and (b) TEMPO@CC and CC.

Nevertheless, after growing HKUST-1 on the Cu mesh, HKUST-1 mesh certainly showed a much higher N^2 sorption and a small hysteresis loop could be also observed, validating that the formation of HKUST-1 enabled Cu mesh to show higher surface area (i.e., 30 m^2/g). On the other hand, N_2 sorption isotherms of pristine CC and TEMPO@CC could be seen in Fig. 5(b), and these two materials exhibited very similar isotherms as the fibrous structure of CC remained after the modifications. Nonetheless,

a slightly higher N_2 sorption was obtained by TEMPO@CC possibly because the acidic pretreatment (by HCl) might roughen the surface of carbon fibers, leading to a slightly higher surface area of 626.8 m^2/g than that of pristine CC (i.e., 558.4 m^2/g).

3.2 Conversion of VAL to VN by the sandwich-like catalytic system

As mentioned in the earlier section, VAL conversion using SCS was implemented by bundling HKUST-1 meshes and TEMPO@CC to form the SCS as displayed in Fig. 6(a), which was hanged by a Cu wire in the center of the reactor as demonstrated in Fig. 6(b). The reactants would then flow through and continuously contact with HKUST-1 meshes and TEMPO@CC as illustrated in Fig. 6(c).

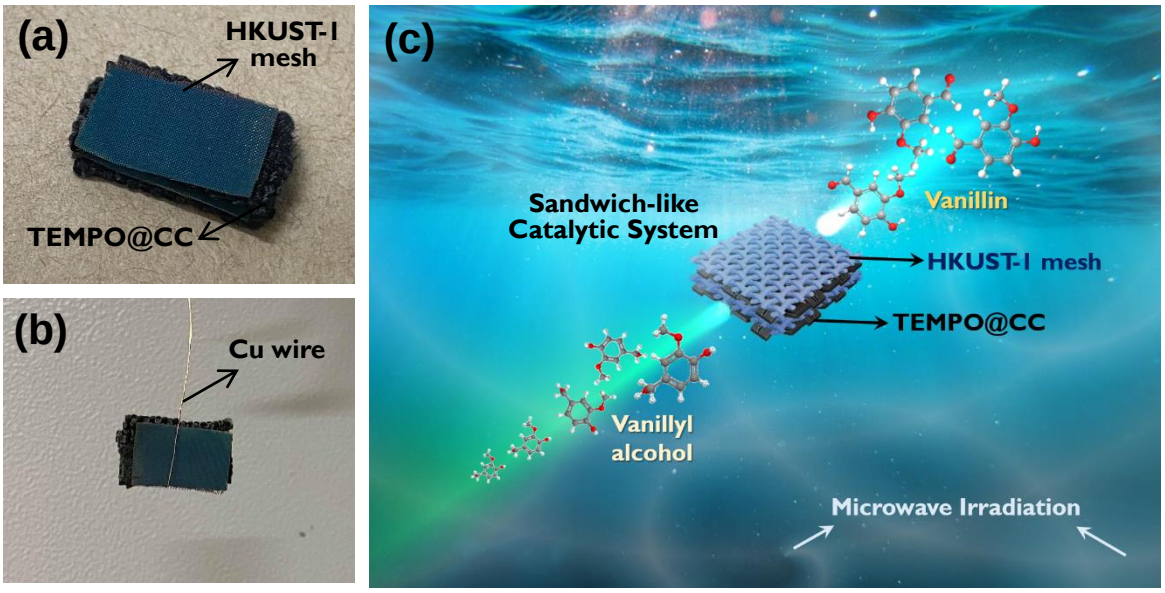

Fig. 6. (a) picture of the sandwich-like catalytic system consisting of inter-stacked HKUST-1 meshes and TEMPO@CC; (b) the sandwich-like catalytic system bundled and hanged by a Cu wire; and (c) illustration of flow-through reaction of VAL converted to VN via the sandwich-like catalytic system under microwave irradiation.

As VAL conversion to VN is a thermo-chemical reaction, heating processes are highly critical. Especially, since SCS consisted of the inter-stacked multilayers of active components, it is important to enable the SCS to achieve desired temperatures. Thus, in

the present study, two distinct heating methods were employed and compared: conventional heating by oven and MWI. Fig. 7(a) firstly shows VAL conversion by HKUST-1 meshes, TEMPO@CC and SCS (HKUST-1 meshes inter-stacked with TEMPO@CC) with COH. When HKUST-1 mesh alone was present, almost no VAL was converted and no VN could be detected.

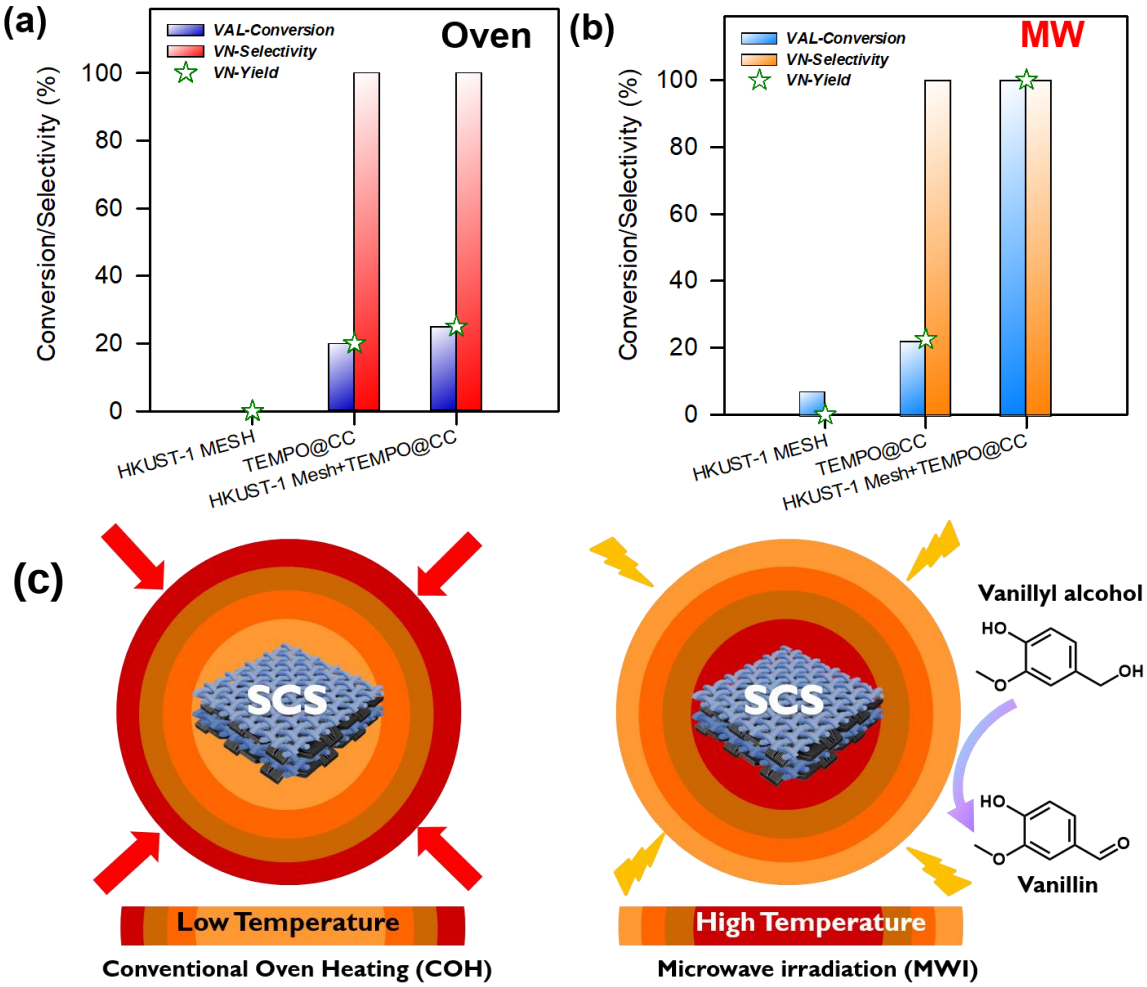

Figure 7. Conversion of VAL to VN using different materials (a) in a conventional oven and (b) under microwave irradiation (VAL = 10mg, IPA = 20 mL, SCS = 0.4 g).

On the other hand, when TEMPO@CC alone was then tested and it was slightly active and capable of a small fraction of VAL (C_{VAL} = 20%) with a very high selectivity for VN. Once TEMPO@CC was combined with HKUST-1 mesh, forming the SCS, C_{VAL} was slightly increased from 20 to 25% and the selectivity still remained very high.

These results demonstrated that TEMPO@CC itself had been active for oxidizing VAL to VN and the SCS could further enhance conversion slightly.

When the heating method was switched to microwave irradiation, HKUST-1 mesh alone seemed still ineffective to convert VAL to VN (Fig. 7(b)). On the other hand, VAL was also successfully converted to VN by TEMPO@CC under MWI and C_{VAL} seemed to increase slightly with MWI. Nevertheless, TEMPO@CC was still insufficient to achieve efficient conversion of VAL. However, once both HKUST-1 mesh and TEMPO@CC were inter-stacked to form SCS under MWI, its corresponding VAL conversion achieved 100% with S_{VN} = 100%, leading to Y_{VN} = 100%. This indicates that SCS was certainly capable of converting VAL to VN with high selectivity and yield, and MWI was powerful to enhance conversion of VAL.

The aforementioned comparison clearly indicates that that the heating method played a critical role for solvothermal reaction of VAL oxidation and MWI was certainly more advantageous than COH as MWI provided a more efficient heating process for rapid and intense heat from the interior of catalyst [49-52]. In particular, as MWI was adopted, the Cu-O group of HKUST-1 could absorb MW and obtain heat much more quickly from the interior of HKUST-1 [53], enabling it much more effective for VAL conversion. More importantly, since Cu-O groups of HKUST-1 were coordinated with the ligand, BTC, BTC would also absorb MWI and promote catalytic activities of Cu-O groups [53]. On the other hand, CC has been also validated as a strong MW absorber and CC should receive heat from the interior much quickly under MWI in contrast to conventional oven heating [54, 55].

Therefore, the enhancement of VAL conversion to VN by SCS under MWI could be ascribed to the feature that the Cu-O group of HKUST-1 and CC were more catalytic active because of fast and intense heat from the core center of catalysts [49, 50]. In

contrast, COH provided the highest temperature on the reactor wall but much lower temperature in the central region [49], resulting in much less effective conversion of VAL as illustrated in Fig. 7(c).

3.3 Effects of reaction temperature and time on VAL conversion by SCS

As VAL conversion to VN is a solvothermal reaction, reaction temperature was extremely critical for VAL oxidation and it would be also useful to investigate VAL conversion at relatively short durations under MWI. Fig. 8(a) displays VAL conversion efficiency as a function of temperature ranging from 60 to 120 °C.

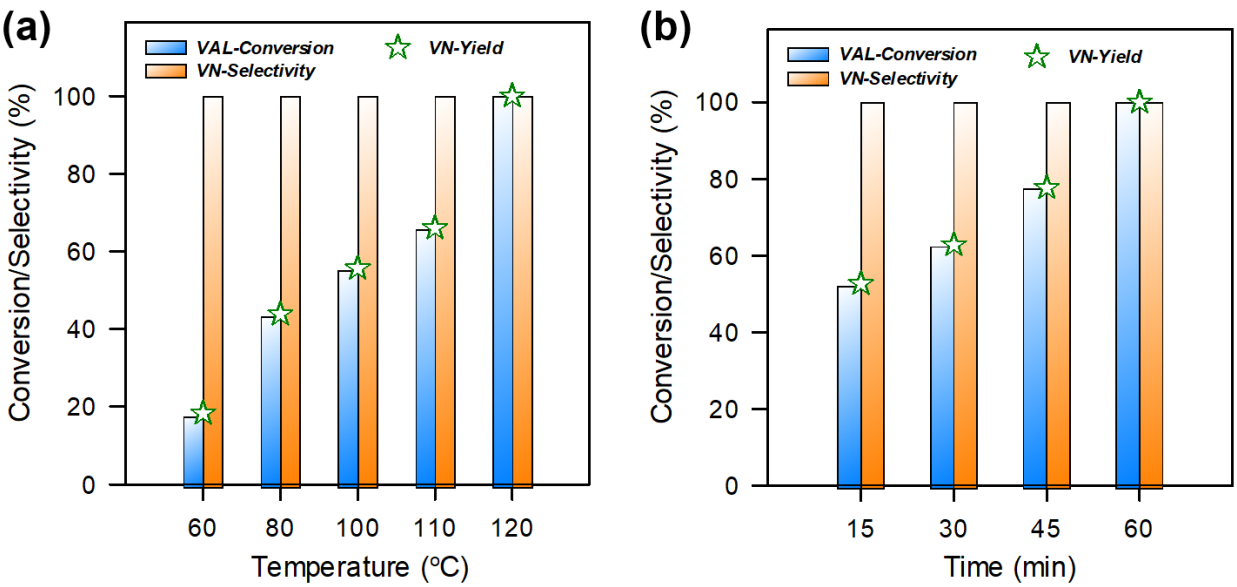

Fig. 8. Effects of (a) temperature (t = 60 min) and (b) time (T = 120 °C) on conversion efficiency of VAL to VN (VAL = 10mg, IPA = 20 mL, SCS = 0.4 g)

When the reaction temperature was low as 60 °C, VAL could be still oxidized to VN with C_{VAL} = 19%. Even though the conversion was relatively low, its corresponding selectivity was still 100%. Once the temperature further increased to 80 °C, C_{VAL} could be then raised to 43% while maintaining S_{VN} = 100%. At higher temperatures of 100,

110 and 120 °C, C_{VAL} further increased to 55, 66 and 100%, respectively, and S_{VN} remained consistent as 100%. This demonstrates that VAL could be also oxidized selectively to VN even at relatively low temperatures. Nevertheless, this result also suggests that temperature was validated as a crucial factor and 120 °C would be an optimal temperature for complete conversion of VAL to VN. Thus, 120 °C was then selected for further investigating effect of reaction duration.

Fig. 8(b) shows VAL conversion efficiency as a function of reaction time ranging from 15 to 60 min. As short as 15 min at 120 °C under MWI, C_{VAL} could reach 53% and S_{VN} was 100%. This signifies that a reaction duration of 15 min under MWI had been capable of converting more than a half of VAL to VN. As the reaction time further increased to 30 and 45 min, C_{VAL} was raised to 63 and 78%, respectively, revealing that a longer reaction time certainly enhanced VAL conversion while S_{VN} remained 100%. Once the reaction duration was extended to 60 min, C_{VAL} could reach 100% and, more importantly, no over-oxidation was observed as no vanillic acid was detected, demonstrating that SCS was highly advantageous and promising for VAL conversion. These results suggest that the optimal condition for VAL conversion by SCS is 120 °C for 60 min under MWI.

To further evaluate competitiveness of SCS for VAL conversion, Table 1 lists VAL conversion efficiencies of reported processes. One can notice that most of reported processes exhibited much lower conversions (ranging from 7 to 96%), and corresponding selectivities (ranging from 5 to 96.5%) and yields (ranging from 1.4 to 92.6%) were also relatively low in comparison to those obtained by SCS. This validates that SCS is certainly more useful than almost all reported systems.

Table 1. VAL to VN catalyzed by using various oxidation techniques.

Catalyst	***Oxidant***	***Temp.(°C)***	***VAL Con. (%)***	***VN Sel.(%)***	***VN Yield(%)***	***Ref.***
SCS	**air**	**120**	**100**	**100**	**100**	**This study**
Cu/TEMPO	air	90	99	93	91	[42]
TEMPO@SiO_2/Cu+	air	30	96	96.5	92.6	[27]
CuO/$MgAl_2O_4$	H_2O_2	90	67	74		[56]
CuO/$MgFe_2O_4$			53	46		
MnFe	O_2	100	21	79	21	[57]
FeFe			70	91	31	
CoFe			70	84	5	
NiFe			76	11	5	
CuFe			86	35	5	
ZnFe			46	19	15	
Au-Pd	air	RT	52.8	49.6	26.2	[58]
N-RGO/Mn_3O_4	air	120	26.4	19.2	5.1	[59]
nCo-MO	air	120	7.0	5.7	0.4	[60]
Co_3O_4	air	120	47.9	60.6	29	[26]
$MnCl_2$	H_2O_2	75	38	19	7.2	[6]
	H_2O_2	75	28	5	1.4	
	H_2O_2	80	89.6	49.4	44.3	
$CrCl_3$	H_2O_2	80	94.2	60.6	57.1	
$CoCl_2$	H_2O_2	80	48.1	33.9	16.3	

3.3 Potential mechanism of VAL conversion by SCS

As SCS was validated to successfully and effectively convert VAL to VN (Fig. 9(a)), it would be interesting to speculate the corresponding conversion mechanism. As SCS was comprised of the inter-stacked HKUST-1 mesh and TEMPO@CC, the Cu-O group of HKUST-1 would firstly react with VAL as illustrated in Fig. 9(b) [61, 62]. Subsequently, TEMPO@CC would then react with the intermediate of VAL to pull out a proton [61, 62], resulting in TEMPOH@CC and the product, VN. The resultant

TEMPOH would be then transformed back to TEMPO via mediation by O_2 [30, 40]. Through these catalytic reactions involving with the Cu-O group, TEMPO and VAL, VAL would be constantly and selectively converted to VAL [63].

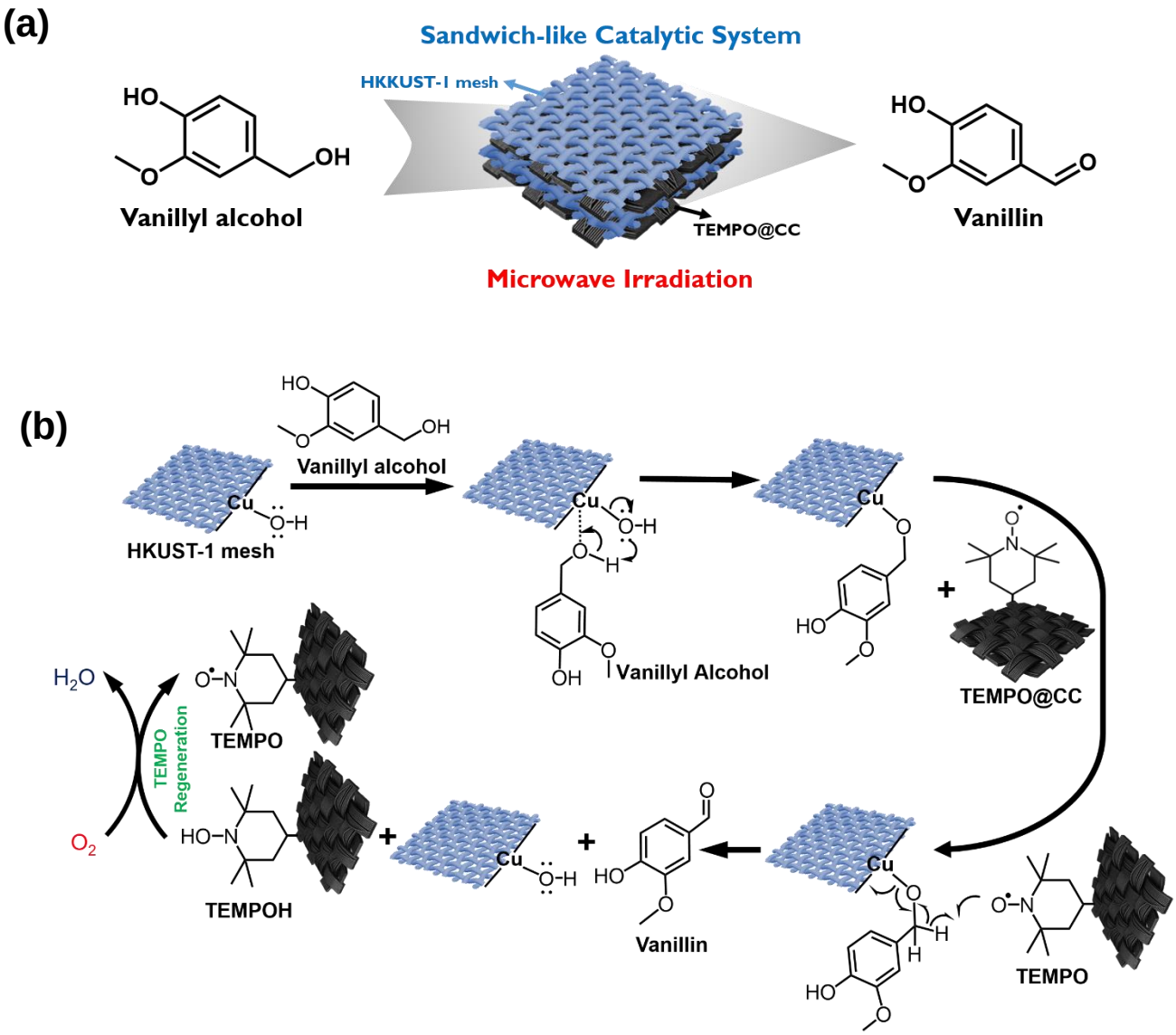

Fig. 9. (a) Illustration of VAL conversion to VN using the sandwich-like catalyst system (SCS), and (b) a proposed mechanism for VAL conversion to VN using the sandwich-like catalyst system (SCS).

3.4 Recyclability of SCS for VAL conversion

As SCS was proposed as a heterogeneous catalytic system, its recyclability would be critical and thus evaluated for multi-cyclic experiments of VAL oxidation. Fig. 10

shows continuous VAL conversion by SCS over 5 cycles and C_{VAL}, S_{VN} and Y_{VN} were remained almost the same (~100%) over the 5 cycles. This demonstrated that the catalytic activities of SCS, which consisted of HKUST-1 mesh and TEMPO@CC, were well retained and remained highly active for VAL conversion, indicating that SCS was stable, efficient and reusable for VAL oxidation to VN.

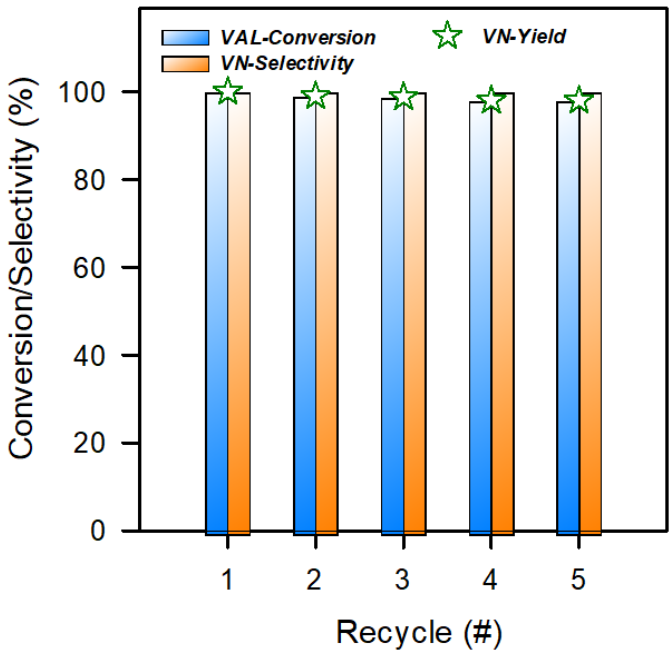

Figure 10. Recyclability of SCS for oxidation of VAL (VAL = 10mg, IPA = 20 mL, SCS = 0.4 g).

The used HKUST-1 mesh and TEMPO@CC can be also seen in Fig. 11(a) and (b), respectively. Their appearances suggested that HKUST-1 crystals were still retained on the surface of Cu mesh and the surface of used carbon fiber was almost unchanged. Furthermore, the XRD pattern of used HKUST-1 mesh (Fig. 11 (c)) was consistent to the theoretical XRD pattern of HKUST-1, indicating that crystalline structures of HKUST-1 remained. On the other hand, ESR analysis was adopted to examine whether TEMPO was retained in TEMPO. Fig. 11 (d) shows that the three-line hyperfine

splitting pattern (attributed to TEMPO) was still detected, validating that TEMPO moieties were preserved in the used TEMPO@CC. These results both demonstrated that SCS was highly stable and reusable for VAL conversion.

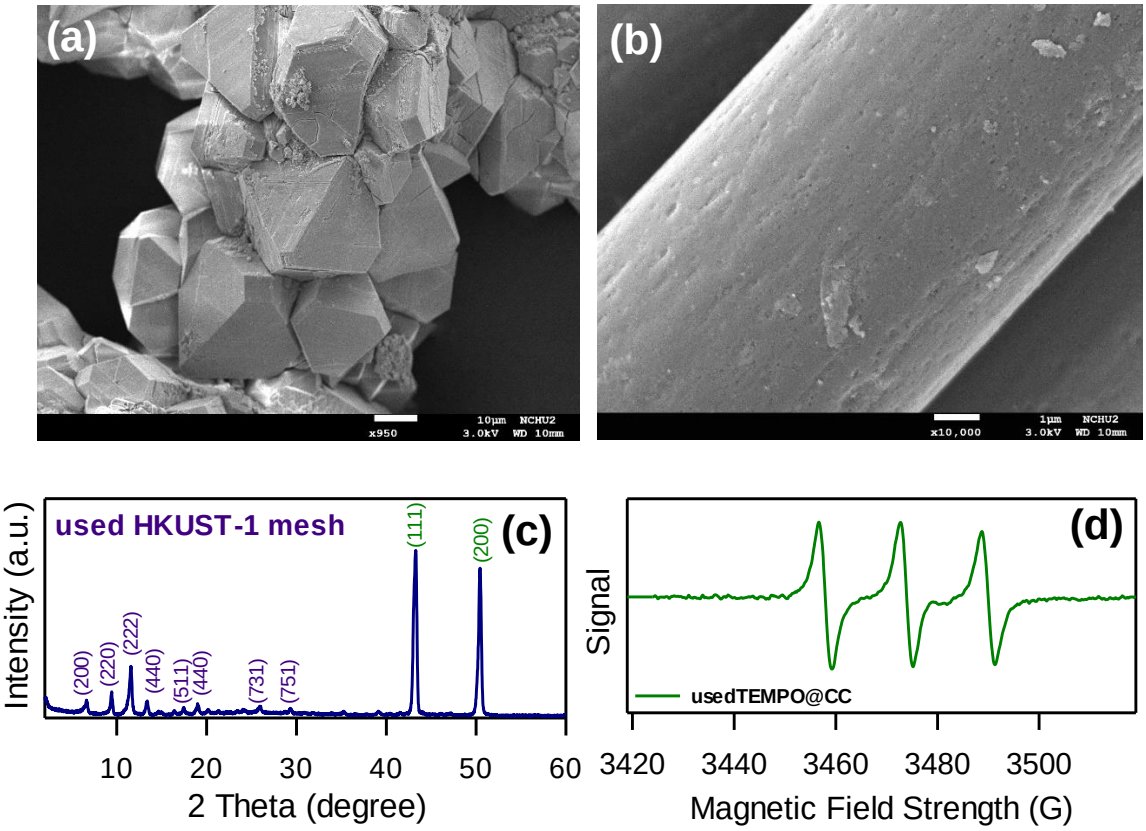

Fig. 11. SEM images of (a) HKUST-1 mesh and (b) TEMPO@CC; (c) XRD pattern of used HKUST-1 mesh and (d) ESR analysis of used TEMPO@CC.

4. Conclusions

In this study, a unique sandwich-like catalytic system (SCS) comprised of HKUST-1 mesh and TEMPO@CC was developed and fabricated as an integrated heterogeneous catalyst for VAL oxidation. Through the electro-chemical technique, Cu mesh was adopted as a source of Cu to grow HKUST-1 directly, whereas CC was functionalized by TEMPO via covalent bonds. These resultant sheet-like materials were then inter-stacked to allow layer-by-layer contacts between HKUST-1 and TEMPO, and flow-thru

reactions of VAL oxidation. Especially, such a SCS exhibited much higher conversion of VAL to VN under MWI than conventional oven heating. SCS was also capable of converting VAL to VN even at relatively low temperature as 60 °C for a very short duration of 15 min. As temperature and reaction time increased, SCS could achieve 100% of conversion, 100% of selectivity and 100% of yield of VN at 120 °C for 60 min. This full conversion of VAL to VN surpassed almost all the reported values by other processes in literature, validating its promising advantages. In addition, SCS could be also reusable and continuously implemented for VAL conversion to VN. The used HKUST-1 mesh could retain crystalline structures of HKUST-1, whereas TEMPO was also preserved on TEMPO@CC, indicating that SCS would be a stable and reusable integrated catalyst for VAL oxidation to VN.

Acknowledgement:

This work is supported by the Ministry of Science and Technology (MOST)(109-2636-E-005-003-), Taiwan, and financially supported by the "Innovation and Development Center of Sustainable Agriculture" from The Featured Areas Research Center Program within the framework of the Higher Education Sprout Project by the Ministry of Education (MOE), Taiwan.

References:

[1] R.D. Perlack, L.L. Wright, A.F. Turhollow, R.L. Graham, B.J. Stokes, D.C. Erbach, Biomass as feedstock for a bioenergy and bioproducts industry: the technical feasibility of a billion-ton annual supply, in: DTIC Document, 2005.

[2] R. Behling, S. Valange, G. Chatel, Heterogeneous catalytic oxidation for lignin valorization into valuable chemicals: what results? What limitations? What trends?, Green Chemistry, 18 (2016) 1839-1854.

[3] H. Lange, S. Decina, C. Crestini, Oxidative upgrade of lignin – Recent routes

reviewed, European Polymer Journal, 49 (2013) 1151-1173.

[4] A. Azarpira, J. Ralph, F. Lu, Catalytic Alkaline Oxidation of Lignin and its Model Compounds: a Pathway to Aromatic Biochemicals, BioEnergy Research, 7 (2014) 78-86.

[5] J. Dai, A.F. Patti, K. Saito, Recent developments in chemical degradation of lignin: catalytic oxidation and ionic liquids, Tetrahedron Letters, 57 (2016) 4945-4951.

[6] J. Pan, J. Fu, X. Lu, Microwave-Assisted Oxidative Degradation of Lignin Model Compounds with Metal Salts, Energy & Fuels, 29 (2015) 4503-4509.

[7] L. Cao, I.K.M. Yu, Y. Liu, X. Ruan, D.C.W. Tsang, A.J. Hunt, Y.S. Ok, H. Song, S. Zhang, Lignin valorization for the production of renewable chemicals: State-of-the-art review and future prospects, Bioresour Technol, 269 (2018) 465-475.

[8] M. Culebras, H. Geaney, A. Beaucamp, P. Upadhyaya, E. Dalton, K.M. Ryan, M.N. Collins, Bio-derived Carbon Nanofibres from Lignin as High-Performance Li-Ion Anode Materials, ChemSusChem, 12 (2019) 4516-4521.

[9] W.J. Liu, H. Jiang, H.Q. Yu, Thermochemical conversion of lignin to functional materials: a review and future directions, Green Chemistry, 17 (2015) 4888-4907.

[10] S. Gharehkhani, Y. Zhang, P. Fatehi, Lignin-derived platform molecules through TEMPO catalytic oxidation strategies, Progress in Energy and Combustion Science, 72 (2019) 59-89.

[11] A. Jha, C.V. Rode, Highly selective liquid-phase aerobic oxidation of vanillyl alcohol to vanillin on cobalt oxide (Co3O4) nanoparticles, New Journal of Chemistry, 37 (2013) 2669-2674.

[12] S. Saha, S.B.A. Hamid, T.H. Ali, Catalytic evaluation on liquid phase oxidation of vanillyl alcohol using air and H2O2 over mesoporous Cu-Ti composite oxide, Applied Surface Science, 394 (2017) 205-218.

[13] A. Jha, D. Mhamane, A. Suryawanshi, S.M. Joshi, P. Shaikh, N. Biradar, S. Ogale, C.V. Rode, Triple nanocomposites of CoMn2O4, Co3O4 and reduced graphene oxide for oxidation of aromatic alcohols, Catalysis Science & Technology, 4 (2014) 1771-1778.

[14] Z. Yuan, S. Chen, B. Liu, Nitrogen-doped reduced graphene oxide-supported Mn3O4: An efficient heterogeneous catalyst for the oxidation of vanillyl alcohol to vanillin, Journal of Materials Science, 52 (2017) 164-172.

[15] S. Ramana, B.G. Rao, P. Venkataswamy, A. Rangaswamy, B.M. Reddy, Nanostructured Mn-doped ceria solid solutions for efficient oxidation of vanillyl alcohol, Journal of Molecular Catalysis A: Chemical, 415 (2016) 113-121.

[16] M. Fache, B. Boutevin, S. Caillol, Vanillin Production from Lignin and Its Use as a Renewable Chemical, ACS Sustainable Chemistry & Engineering, 4 (2016) 35-46.

[17] J.-Y. Lin, H.-K. Lai, K.-Y.A. Lin, Rapid microwave-hydrothermal conversion of lignin model compounds to value-added products via catalytic oxidation using metal organic frameworks, Chemical Papers, (2018).

[18] K.-Y.A. Lin, H.-K. Lai, Z.-Y. Chen, Selective generation of vanillin from catalytic oxidation of a lignin model compound using ZIF-derived carbon-supported cobalt nanocomposite, J Taiwan Inst Chem Eng, (2017).

[19] J. Pan, J. Fu, S. Deng, X. Lu, Microwave-Assisted Degradation of Lignin Model Compounds in Imidazolium-Based Ionic Liquids, Energy & Fuels, 28 (2014) 1380-1386.

[20] J.A.G.d. Silveira, É.M.L. Rabelo, P.C.S. Lima, B.N. Chaves, M.F.B. Ribeiro, Post-mortem hemoparasite detection in free-living Brazilian brown brocket deer (Mazama gouazoubira, Fischer 1814), Revista Brasileira de Parasitologia Veterinária, 23 (2014) 206-215.

[21] R. Yepez, S. Garcia, P. Schachat, M. Sanchez-Sanchez, J.H. Gonzalez-Estefan, E. Gonzalez-Zamora, I.A. Ibarra, J. Aguilar-Pliego, Catalytic activity of HKUST-1 in the oxidation of trans-ferulic acid to vanillin, New Journal of Chemistry, 39 (2015) 5112-5115.

[22] E. Sánchez-González, A. López-Olvera, O. Monroy, J. Aguilar-Pliego, J. Gabriel Flores, A. Islas-Jácome, M.A. Rincón-Guevara, E. González-Zamora, B. Rodríguez-Molina, I.A. Ibarra, Synthesis of vanillin via a catalytically active Cu(ii)-metal organic polyhedron, CrystEngComm, 19 (2017) 4142-4146.

[23] P. Elamathi, M.K. Kolli, G. Chandrasekar, Catalytic Oxidation of Vanillyl Alcohol Using FeMCM-41 Nanoporous Tubular Reactor, International Journal of Nanoscience, 17 (2017).

[24] R. Yepez, J.F. Illescas, P. Gijon, M. Sanchez-Sanchez, E. Gonzalez-Zamora, R. Santillan, J.R. Alvarez, I.A. Ibarra, J. Aguilar-Pliego, HKUST-1 as a Heterogeneous Catalyst for the Synthesis of Vanillin, J Vis Exp, (2016).

[25] J.G. Flores, E. Sánchez-González, A. Gutiérrez-Alejandre, J. Aguilar-Pliego, A. Martínez, T. Jurado-Vázquez, E. Lima, E. González-Zamora, M. Díaz-García, M. Sánchez-Sánchez, I.A. Ibarra, Greener synthesis of Cu-MOF-74 and its catalytic use for the generation of vanillin, Dalton Transactions, 47 (2018) 4639-4645.

[26] R. Behling, G. Chatel, S. Valange, Sonochemical oxidation of vanillyl alcohol to vanillin in the presence of a cobalt oxide catalyst under mild conditions, Ultrasonics Sonochemistry, 36 (2017) 27-35.

[27] M.-W. Zheng, K.-Y.A. Lin, C.-H. Lin, TEMPO-Functionalized Silica as an Efficient and Recyclable Oxidation Catalyst for Conversion of a Lignin Model Compound to Value-Added Products, Waste and Biomass Valorization, (2019).

[28] J.-Y. Lin, J. Lee, K.-Y.A. Lin, Microwave-Assisted Catalyst-Free Oxidative

Conversion of a Lignin Model Compound to Value-Added Products Using TEMPO, Waste and Biomass Valorization, (2019).

[29] A.J. Fatiadi, R. Schaffer, An Improved Procedure for Synthesis of DL-4-Hydroxy-3-methoxymandelic Acid (DL-"Vanillyl"-mandelic Acid, VMA), J Res Natl Bur Stand A Phys Chem, 78A (1974) 411-412.

[30] P.D. Sainsbury, E.M. Hardiman, M. Ahmad, H. Otani, N. Seghezzi, L.D. Eltis, T.D.H. Bugg, Breaking Down Lignin to High-Value Chemicals: The Conversion of Lignocellulose to Vanillin in a Gene Deletion Mutant of Rhodococcus jostii RHA1, ACS Chemical Biology, 8 (2013) 2151-2156.

[31] H.P. Chen, M. Chow, C.C. Liu, A. Lau, J. Liu, L.D. Eltis, Vanillin catabolism in Rhodococcus jostii RHA1, Applied and environmental microbiology, 78 (2012) 586-588.

[32] L. Yan, P. Chen, S. Zhang, S. Li, X. Yan, N. Wang, N. Liang, H. Li, Biotransformation of ferulic acid to vanillin in the packed bed-stirred fermentors, Scientific Reports, 6 (2016) 34644.

[33] A. Converti, B. Aliakbarian, J.M. Domínguez, G. Bustos Vázquez, P. Perego, Microbial production of biovanillin, Braz J Microbiol, 41 (2010) 519-530.

[34] Z. Yuan, B. Liu, P. Zhou, Z. Zhang, Q. Chi, Aerobic oxidation of biomass-derived 5-hydroxymethylfurfural to 2,5-diformylfuran with cesium-doped manganese dioxide, Catalysis Science & Technology, 8 (2018) 4430-4439.

[35] K.-Y.A. Lin, H.-K. Lai, Z.-Y. Chen, Selective generation of vanillin from catalytic oxidation of a lignin model compound using ZIF-derived carbon-supported cobalt nanocomposite, Journal of the Taiwan Institute of Chemical Engineers, 78 (2017) 337-343.

[36] H.-K. Lai, Y.-Z. Chou, M.-H. Lee, K.-Y.A. Lin, Coordination polymer-derived cobalt nanoparticle-embedded carbon nanocomposite as a magnetic multi-functional catalyst for energy generation and biomass conversion, Chemical Engineering Journal, 332 (2018) 717-726.

[37] S. Saha, S.B. Abd Hamid, Nanosized spinel Cu-Mn mixed oxide catalyst prepared via solvent evaporation for liquid phase oxidation of vanillyl alcohol using air and H2O2, RSC Adv, 6 (2016) 96314-96326.

[38] M. Shilpy, M.A. Ehsan, T.H. Ali, S.B. Abd Hamid, M.E. Ali, Performance of cobalt titanate towards H2O2 based catalytic oxidation of lignin model compound, RSC Adv, 5 (2015) 79644-79653.

[39] J.M. Hoover, S.S. Stahl, Highly Practical Copper(I)/TEMPO Catalyst System for Chemoselective Aerobic Oxidation of Primary Alcohols, J Am Chem Soc, 133 (2011) 16901-16910.

[40] N.J. Hill, J.M. Hoover, S.S. Stahl, Aerobic Alcohol Oxidation Using a

Copper(I)/TEMPO Catalyst System: A Green, Catalytic Oxidation Reaction for the Undergraduate Organic Chemistry Laboratory, Journal of Chemical Education, 90 (2013) 102-105.

[41] J.M. Hoover, B.L. Ryland, S.S. Stahl, Mechanism of Copper(I)/TEMPO-Catalyzed Aerobic Alcohol Oxidation, J Am Chem Soc, 135 (2013) 2357-2367.

[42] J.-Y. Lin, K.-Y.A. Lin, Catalytic conversion of a lignin model compound to value-added products using Cu/TEMPO-catalyzed aerobic oxidation, Biomass Conversion and Biorefinery, 9 (2019) 617-623.

[43] S. Barna, E. Ott, T. Nguyen, M. Shannon, A. Scheeline, Silica Adsorbents and Peroxide Functionality for Removing Paraquat from Wastewater, Journal of Environmental Engineering, 139 (2013) 975-985.

[44] B.L. Ryland, S.S. Stahl, Practical Aerobic Oxidations of Alcohols and Amines with Homogeneous Copper/TEMPO and Related Catalyst Systems, Angewandte Chemie International Edition, 53 (2014) 8824-8838.

[45] T.S. Hansen, I. Sádaba, E.J. García-Suárez, A. Riisager, Cu catalyzed oxidation of 5-hydroxymethylfurfural to 2,5-diformylfuran and 2,5-furandicarboxylic acid under benign reaction conditions, Applied Catalysis A: General, 456 (2013) 44-50.

[46] D.L. Pavia, G.M. Lampman, G.S. Kriz, J.A. Vyvyan, Introduction to Spectroscopy, Cengage Learning, 2008.

[47] R. Luo, M. Li, C. Wang, M. Zhang, M.A. Nasir Khan, X. Sun, J. Shen, W. Han, L. Wang, J. Li, Singlet oxygen-dominated non-radical oxidation process for efficient degradation of bisphenol A under high salinity condition, Water Research, 148 (2019) 416-424.

[48] K.C. Das, C.K. Das, Thioredoxin, a Singlet Oxygen Quencher and Hydroxyl Radical Scavenger: Redox Independent Functions, Biochemical and Biophysical Research Communications, 277 (2000) 443-447.

[49] Z.M.A. Bundhoo, Microwave-assisted conversion of biomass and waste materials to biofuels, Renewable and Sustainable Energy Reviews, 82 (2018) 1149-1177.

[50] P. Chen, Q. Xie, Z. Du, F.C. Borges, P. Peng, Y. Cheng, Y. Wan, X. Lin, Y. Liu, R. Ruan, Microwave-Assisted Thermochemical Conversion of Biomass for Biofuel Production, in: Z. Fang, J.R.L. Smith, X. Qi (Eds.) Production of Biofuels and Chemicals with Microwave, Springer Netherlands, Dordrecht, 2015, pp. 83-98.

[51] Z. Zhang, Z.K. Zhao, Microwave-assisted conversion of lignocellulosic biomass into furans in ionic liquid, Bioresour Technol, 101 (2010) 1111-1114.

[52] C. Li, Z. Zhang, Z.K. Zhao, Direct conversion of glucose and cellulose to 5-hydroxymethylfurfural in ionic liquid under microwave irradiation, Tetrahedron Letters, 50 (2009) 5403-5405.

[53] T.-Y. Lin, K.-Y.A. Lin, Microwave-enhanced catalytic transfer hydrogenation of

levulinic acid to γ-valerolactone using zirconium-based metal organic frameworks: A comparative study with conventional heating processes, Journal of the Taiwan Institute of Chemical Engineers, 96 (2019) 321-328.

[54] N. Zhao, T. Zou, C. Shi, J. Li, W. Guo, Microwave absorbing properties of activated carbon-fiber felt screens (vertical-arranged carbon fibers)/epoxy resin composites, Materials Science and Engineering: B, 127 (2006) 207-211.

[55] W. Ye, W. Li, Q. Sun, J. Yu, Q. Gao, Microwave absorption properties of lightweight and flexible carbon fiber/magnetic particle composites, RSC Adv, 8 (2018) 24780-24786.

[56] B. Rahmanivahid, M. Pinilla-de Dios, M. Haghighi, R. Luque, Mechanochemical Synthesis of CuO/MgAl2O4 and MgFe2O4 Spinels for Vanillin Production from Isoeugenol and Vanillyl Alcohol, Molecules, 24 (2019).

[57] M.-W. Zheng, H.-K. Lai, K.-Y.A. Lin, Valorization of Vanillyl Alcohol by Pigments: Prussian Blue Analogue as a Highly-Effective Heterogeneous Catalyst for Aerobic Oxidation of Vanillyl Alcohol to Vanillin, Waste and Biomass Valorization, (2018) 1-10.

[58] M. Wu, J.-H. Pang, P.-P. Song, J.-J. Peng, F. Xu, Q. Li, X.-M. Zhang, Visible light-driven oxidation of vanillyl alcohol in air with Au–Pd bimetallic nanoparticles on phosphorylated hydrotalcite, New Journal of Chemistry, 43 (2019) 1964-1971.

[59] Z. Yuan, S. Chen, B. Liu, Nitrogen-doped reduced graphene oxide-supported Mn3O4: An efficient heterogeneous catalyst for the oxidation of vanillyl alcohol to vanillin, Journal of Materials Science, 52 (2016) 164-172.

[60] A. Jha, D. Mhamane, A. Suryawanshi, S.M. Joshi, P. Shaikh, N. Biradar, S. Ogale, C.V. Rode, Triple nanocomposites of CoMn2O4, Co3O4 and reduced graphene oxide for oxidation of aromatic alcohols, Catalysis Science & Technology, 4 (2014).

[61] A. Dhakshinamoorthy, M. Alvaro, H. Garcia, Aerobic Oxidation of Benzylic Alcohols Catalyzed by Metal−Organic Frameworks Assisted by TEMPO, ACS Catalysis, 1 (2010) 48-53.

[62] N.J. Hill, J.M. Hoover, S.S. Stahl, Aerobic Alcohol Oxidation Using a Copper(I)/TEMPO Catalyst System: A Green, Catalytic Oxidation Reaction for the Undergraduate Organic Chemistry Laboratory, Journal of Chemical Education, 90 (2012) 102-105.

[63] W.-C. Yun, T.-Y. Lin, H.-Y. Chiu, K.-Y.A. Lin, Microwave Irradiation-Enhanced Catalytic Transfer Hydrogenation of Levulinic Acid to γ-Valerolactone Using Ruthenium: A Comparative Study with Conventional Heating Processes, Waste and Biomass Valorization, (2019).

Marked-up Revised Manuscript Click here to view linked References

Integrated MOF-mesh and TEMPO-grafted Carbon Fiber as a Sandwich-like Catalytic System for Selective Valorization of Lignin-derived Compound under Microwave Irradiation

Jia-Yin Lin[a], *Haitao Wang*[b], *Wen Da Oh*[c], *Jechan Lee*[d], *Eilhann Kwon*[e], *Siming You*[f], *Chia-Hua Lin*[g,*], *and Kun-Yi Andrew Lin*[a,*]

[a]Department of Environmental Engineering & Innovation and Development Center of Sustainable Agriculture & Research Center of Sustainable Energy and Nanotechnology, National Chung Hsing University, 250 Kuo-Kuang Road, Taichung, Taiwan

[b]Key Laboratory of Pollution Processes and Environmental Criteria, College of Environmental Science and Engineering, *Nankai University*, Tianjin 300071, P. R. China

[c]School of Chemical Sciences, Universiti Sains Malaysia, 11800 Penang, Malaysia

[d]Department of Environmental and Safety Engineering, *Ajou University*, Suwon 16499, Republic of Korea

[e]Department of Environment and Energy, Sejong University, 209 Neungdong-ro, Gunja-dong, Gwangjin-gu, Seoul, Republic of Korea

[f]James Watt School of Engineering, University of Glasgow, Glasgow G12 8QQ, UK

[g]Department of Biotechnology, National Formosa University, Yunlin 63208, Taiwan

*Corresponding Authors. E-mail address: linky@nchu.edu.tw (K.-Y. A. Lin); sptong@zjut.edu.cn (Shaoping Tong)

Abstract

Oxidation of vanillyl alcohol to vanillin represents a critical step towards sustainable valorization of lignocellulosic biomass. Although catalytic oxidation of vanillyl alcohol by Cu and 2,2,6,6-tetramethylpiperidine 1-oxyl (TEMPO) is promising for vanillyl alcohol oxidation, the traditional Cu/TEMPO adopts homogeneous Cu ions and TEMPO, which are difficult for recovery and reuse. In this study, a unique sandwich-like catalytic system (SCS), which comprises HKUST-1 mesh and TEMPO-grafted on carbon cloth, is developed as a heterogeneous catalyst for vanillyl alcohol oxidation. Through the electro-chemical technique, copper (Cu) mesh is used as a source of Cu to grow HKUST-1 directly, whereas carbon cloth is functionalized by TEMPO via covalent bonds. These resultant materials are then stacked to achieve layer-by-layer contacts between HKUST-1 and TEMPO, and enable flow-through reactions of VAL oxidation. Especially, such a SCS exhibits much higher conversion of vanillyl alcohol to vanillin under microwave irradiation than conventional oven heating. SCS could achieve 100% of conversion, 100% of selectivity and 100% of yield of vanillin at 120 °C for 60 min. This full conversion of vanillyl alcohol to vanillin surpasses almost all the reported values by other processes in literature, and SCS could be also reusable and continuously implemented for vanillyl alcohol conversion to vanillin. The used HKUST-1 mesh could retain crystalline structures of HKUST-1, whereas TEMPO is also preserved on TEMPO@CC, indicating that SCS would be a stable and reusable integrated catalyst for vanillyl alcohol oxidation to vanillin.

Keywords: hybrid mesh, MOFs, HKUST-1, carbon cloth, lignin, vanillyl alcohol, vanillin

1. Introduction

Lignocellulosic biomass and biowaste are considered as a renewable resource which can be further utilized and valorized [1, 2]. Many approaches have been proposed for valorizing lignocellulosic biomass, such as pyrolysis and oxidation [3-8]. Although pyrolysis can rapidly decompose biomass to several products, chars from pyrolysis remain as a challenging issue and many other issues still exist at large-scale operations [9, 10]. In contrast, oxidation of lignocellulosic biomass seems a more feasible and favorable approach as oxidation processes are milder and more environmentally benign [6, 11-15]. More importantly, oxidation of lignin-derived molecules can generate many valuable compounds with versatile functions [10].

As lignin contains relatively complex structures, oxidation processes are usually investigated by oxidizing lignin-derived model compounds [2, 5, 6, 16-19]. As the *β*-O-4 has been regarded as the most typical sub-structure of lignin [20], decomposition of these *β*-O-4 sub-structures of lignin produces several low-molecular-weight derivatives. Among these lignin-derived molecules, such as 3-methoxy-4-hydroxycinnamic acid [21-25], and vanillyl alcohol (VAL) [16, 26-28], VAL is particularly attractive as oxidation of VAL can produce a high-value-added compound, vanillin (VN), which is a widely-consumed flavorant used in foods, perfumes, cosmetics, pharmaceuticals and drinks [16]. Conventionally, vanillin is extracted from *Vanilla planifolia*; however chemical synthesis of vanillin has become a dominant source because of vast demand of vanillin. To date, one of the most popular route for synthesizing vanillin requires usage of petrochemical raw chemical, guaiacol, through multiple steps [29]. Recently, biological production of vanillin has been also proposed by using bacteria (e.g., *Rhodococcus jostii* RHA1) through decomposition of lignin into vanillin [30, 31] and fermentation of ferulic acid [32, 33].

Even though a few studies have converted VAL to VN via oxidation, these researches employed un-recyclable oxidant, H_2O_2, [34-36] and a large amount of H_2O_2 is required because of stoichiometric chemistry. More importantly, these H_2O_2-based oxidation methods usually lead to very low conversion of VAL (C_{VAL}), selectivity for VN (S_{VN}) and yield of VN (S_{VN}) [6, 18, 37, 38].

Since recent interests of oxidative reactions are focused on utilization of oxygen gas molecules (O_2) as a direct oxidant [39-41], it would be certainly sustainable to develop a process of VAL conversion by using O_2 to oxidize VAL to VN. To this end, an useful oxidation process of utilizing O_2, especially for oxidation of alcohols, is revealed by using Cu as a metal catalyst and 2,2,6,6-tetramethylpiperidine 1-oxyl (TEMPO) as an organic oxidation co-catalyst together with O_2 as an oxidant [42]. The integration of Cu/TEMPO has been validated as an effective catalytic system for oxidizing alcohols to corresponding aldehydes [39-41, 43, 44]. As VAL is an alcohol, which can be further oxidized to produce an aldehyde group, forming VN, The integration of Cu/TEMPO would be useful for VAL oxidation.

Nevertheless, the traditional integration of Cu/TEMPO uses homogeneous Cu ions and TEMPO [45] but recovering Cu ion and TEMPO from reactions is certainly highly-challenging. To address the aforementioned issue, it would be critical to develop heterogeneous catalysts containing Cu and TEMPO moieties. Moreover, these heterogeneous catalysts must be easily implemented, recovered and reused. Even though powders and particles (or nanoparticles) are promising catalysts, fine powders/particles are actually still difficult to recover and reuse. Thus, macroscale substrate-supported catalysts, on which nanoscale active components or molecular compounds are deposited, would be advantageous because marco-substrates allow them to be easily operated and nanoscale active components would provide high

activities. Among various types of macroscale substrates, mesh-like substrates would be highly favorable as they can be grafted with nanoscale components but still allow reactants to flow-through these mesh-like substrates for target reactions. To this end, the present study proposes to develop mesh-supported catalysts containing Cu and TEMPO. In the case of Cu-containing mesh, while Cu mesh is readily available, Cu mesh exhibits very low surface areas and active sites. Therefore, Cu-based metal organic frameworks (MOFs) is then particularly fabricated by direct growth of Cu-MOFs (i.e., HKUST-1) on Cu mesh, which not only acts as a support but also serves as a Cu source to grow HKUST-1. On the other hand, TEMPO would be grafted on a stable and robust mesh-like substrate, carbon cloth (CC), via covalent bonds. The resultant HKUST-1 mesh and TEMPO@CC would be inter-stacked to form a sandwich-like catalytic system (SCS) for allowing layer-by-layer contacts between Cu and TEMPO. Once reactants (i.e., VAL) flow through this SCS, VAL would react with Cu and then TEMPO continuously to transform into VN.

Moreover, as such a reaction of VAL oxidation is a solvothermal reaction, heating processes have been a key to conversion efficiencies. In this study, conventional oven heating (COH) and microwave irradiation (COH) have been also adopted and compared for VAL conversion by SCS. To our best knowledge, such a SCS or hybrid-mesh catalysts have been never reported for VAL conversion and thus fabrication techniques and corresponding catalytic behaviors given here would be highly useful and insightful.

2. Experimental

2.1 Materials

All chemicals employed in this study were of analytical-regent grade and were used without further purification. Cu mesh (100 mesh, 99.9% copper) was purchased from

May Chun Company Limited (Taiwan). Carbon cloth (CC) was provided by Taicarbon Company (Taiwan). Copper (II) nitrate trihydrate (Cu $(NO_3)_2 \cdot 3H_2O$) and iso-propanol (IPA) were obtained from Union Chemicals (Taiwan), whereas benzene-1,3,5-tricarboxylic acid (H_3BTC) was purchased from Showa Chemical Co. Ltd (Taiwan), and 4-Hydroxy-TEMPO was received from Merck (Germany). Tetrahydrofuran and N,N'-dicyclohexylcarbodiimide were purchased from Sigma-Aldrich (USA).

2.2 Preparation of HKUST-1 MESH

A piece of Cu mesh (0.5 cm × 1 cm) with a thickness of 0.1mm was immersed in 3M HCl and placed in an ultrasound bath for 15 min to remove its surficial impurities followed by rinsing it with DI water and ethanol. Next, Cu mesh was used as anode, whereas titanium plate (99.9% Titanium) was used as the cathode. A mixture of ethanol and DI water (1:1) was then employed as the electrolyte to which 100 mg H_3BTC was directly added. Subsequently, the anodizing growth of HKUST-1 mesh was carried out at 5V for 20 min at room temperature as illustrated in Fig. 1(a). The resultant HKUST-1 mesh was then rinsed with ethanol and DI water thoroughly and dried at 80 °C in oven for 12h to afford HKUST-1 mesh.

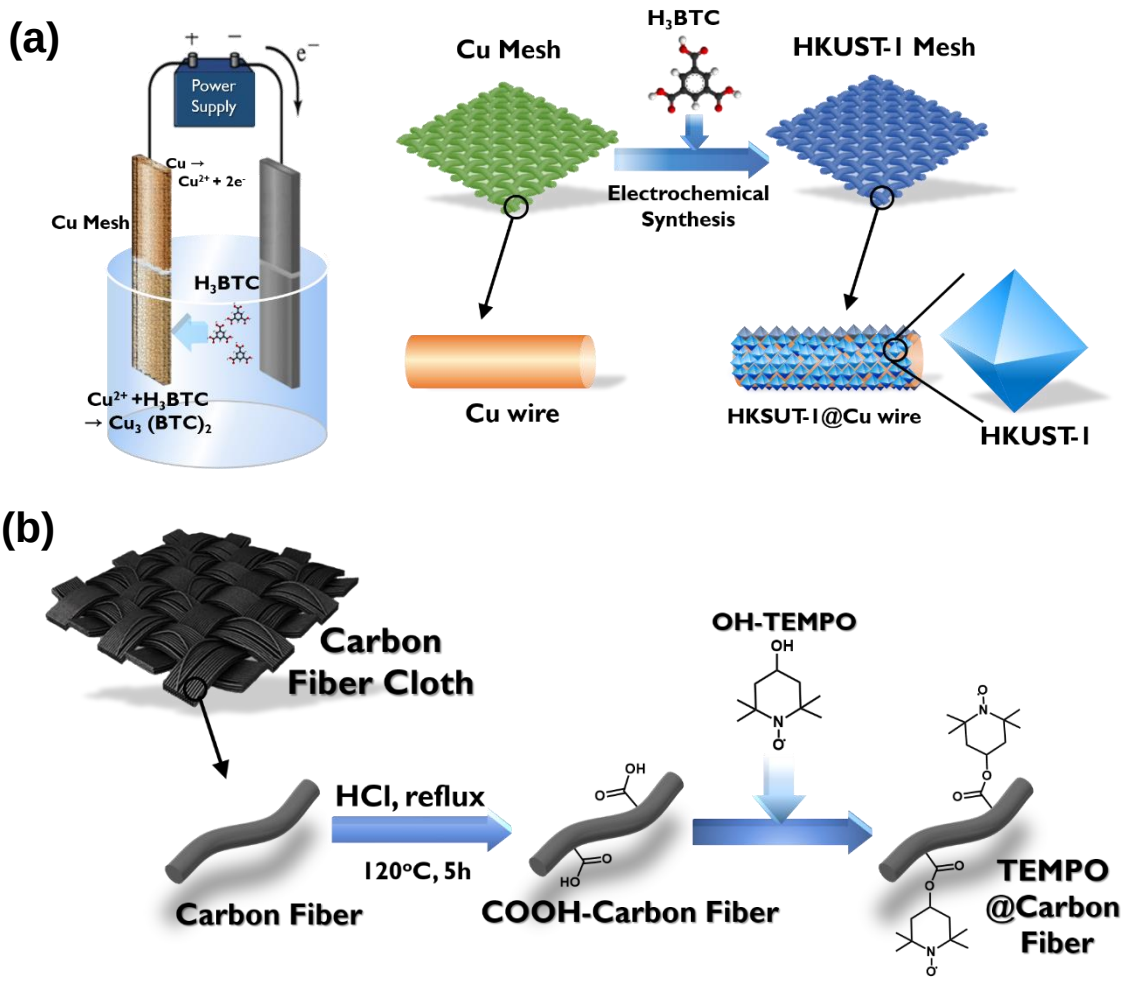

Figure 1. Schematic illustrations for preparation of (a) HKUST-1 mesh via the one-step electrochemical synthesis and (b) TEMPO@CC

2.3 Synthesis of TEMPO@CC

The synthetic route for TEMPO@CC could be illustrated in Fig. 1(b). Firstly, a piece of CC (0.5 cm × 1 cm) was added in a flask with 50 mL of HCl and 100 mL of DI water. Then, the mixture flask with a condenser was placed on a temperature-controllable stirring plate. The resulting mixture was refluxed for 5h under 110oC. After cooling temperature to 40 °C, the acid-treated carbon cloth was washed with DI water repeatedly and dried in oven at 80 °C overnight. This resultant carboxyl-functionalized CC, together with OH-TEMPO (0.4 g) and N,N'-dicyclohexylcarbodiimide (0.578 g)

were then mixed in 20 mL of tetrahydrofuran at ambient temperature for 72 hours. Finally, the TEMPO-grafted CC (i.e., TEMPO@CC) was washed with methanol/DI water and then dried at 80oC in oven overnight. Electron spin resonance (ESR) spectrum of TEMPO@CC was implemented by a Bruker EMX Plus X-Band spectrometer.

2.4 Conversion of VAL to VN

Catalytic conversion of VAL was implemented in a cylindrical Teflon-lined reactor in which the bundled sandwich-like catalyst (two HKUST-1 meshes inter-stacked with two TEMPO@CC) was hanged and suspended in the center of the reactor to allow reactants to flow through. In a typical experiment, 10 mg of VAL and 20 mL of iso-propanol were added to the Teflon-lined reactor. Next, the mixture was then heated by MWI or in a conventional oven to start VAL conversion. The MWI system was Ethos UP (Milestone, Italy) whose volume was 70 liters with two 950 watt magnetrons and its temperature range is from the ambient temperature to 220 °C. The conventional oven used in this study was Memmert (Germany), ULE 400, whose volume was 53 liters and temperature range is from 30 to 220 °C with natural convection. After pre-set reaction times, sample aliquots were withdrawn from the vessel and filtrated through syringe membrane disks (0.22 μm, PVDF). The filtrates were analyzed for concentrations of reactant and products using a HPLC (Kanuer Azura, Germany) with a UV-Vis detector (275 nm) and a reverse-phase C-18 column. The mobile phase consisted of aqueous acetonitrile (20%), acetic acid (1%) and distilled water (79%) at a flowrate of 1.0 mL/min.

Based on previous literatures [4, 34], chemical oxidation of VAL to VN was quantified as follows:

$$\text{Conversion of VAL } (C_{VAL}) = \frac{\text{Consumed VAL}}{\text{Total VAL}} \times 100\% \quad (1)$$

$$\text{Selectivity for VN } (S_{VN}) = \frac{\text{VN (mol)}}{\text{Consumed VAL (mol)}} \times 100\% \quad (2)$$

$$\text{Yield } (Y_{VN}) = \frac{\text{VN (mol)}}{\text{Total VAL (mol)}} \times 100\% \quad (3)$$

3. Results and discussion

3.1 Characterization of HKUST-1 mesh and TEMPO@CC

To characterize HKUST-1 mesh, the picture of pristine Cu mesh was firstly revealed in Fig. 2(a) and it exhibited the very typical reddish brown color. Fig. 2(b) and (c) further show that the pristine Cu mesh was extremely smooth. After the anodic growth of HKUST-1 on the Cu mesh, the color of the mesh had completely changed from reddish brown to blue as seen in Fig. 2(a). Another noteworthy feature was that the blue color was very homogeneous all over the entire piece, suggesting that the electro-chemical technique was certainly capable of growing HKUST-1 on the mesh. Closer views (Fig. 2(d) and (e)) further reveal that the originally smooth surface of mesh had been modified, and fully and uniformly covered by octahedral crystals. This octahedral morphology was consistent to the typical morphology of HKUST-1, suggesting that HKUST-1 was successfully grown on the Cu mesh.

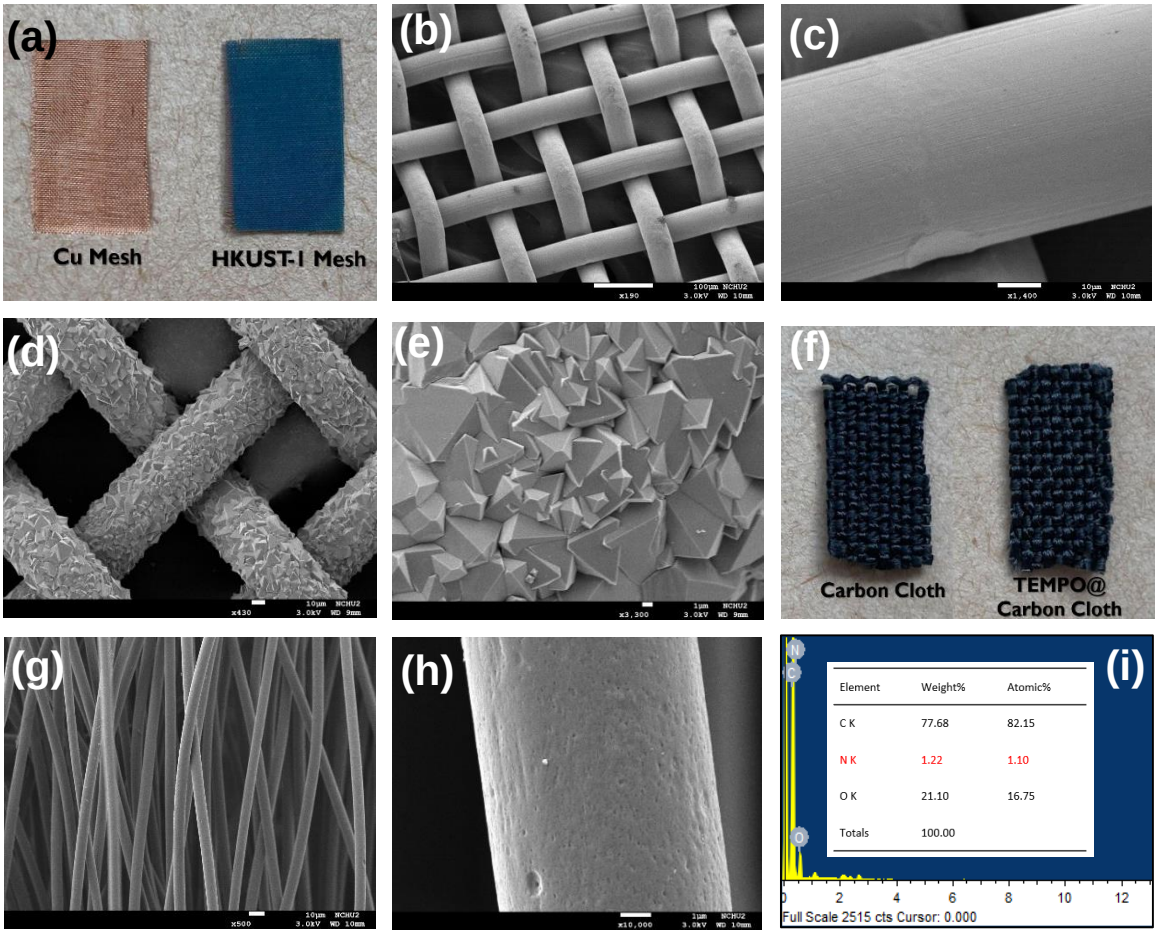

Fig. 2. (a) Pictures of Cu mesh and HKUST-1 mesh; SEM images of (b), (c) pristine Cu mesh; (d), (e) HKUST-1 mesh; (f) pictures of carbon cloth and TEMPO@CC; (g),(h) SEM image of TEMPO@CC; and (i) EDS analysis of TEMPO@CC.

Fig. 3(a)-(d) further display the elemental mapping result of this HKUST-1 mesh and elements of C, O and Cu were easily detected and evenly distributed all over the mesh, demonstrating that the Cu mesh had been completely and homogeneously covered by HKUST-1. Fig. 4(a) also confirms that after the anodizing Cu mesh with H_3BTC, the XRD pattern of Cu mesh had changed significantly to exhibit a series of peaks ranging from 5 to 45 °, which were in line with the signature peaks of HKUST-1, validating that HKUST-1 was certainly and successfully grown on the mesh.

On the other hand, pictures of CC and the TEMPO-grafted CC were displayed in

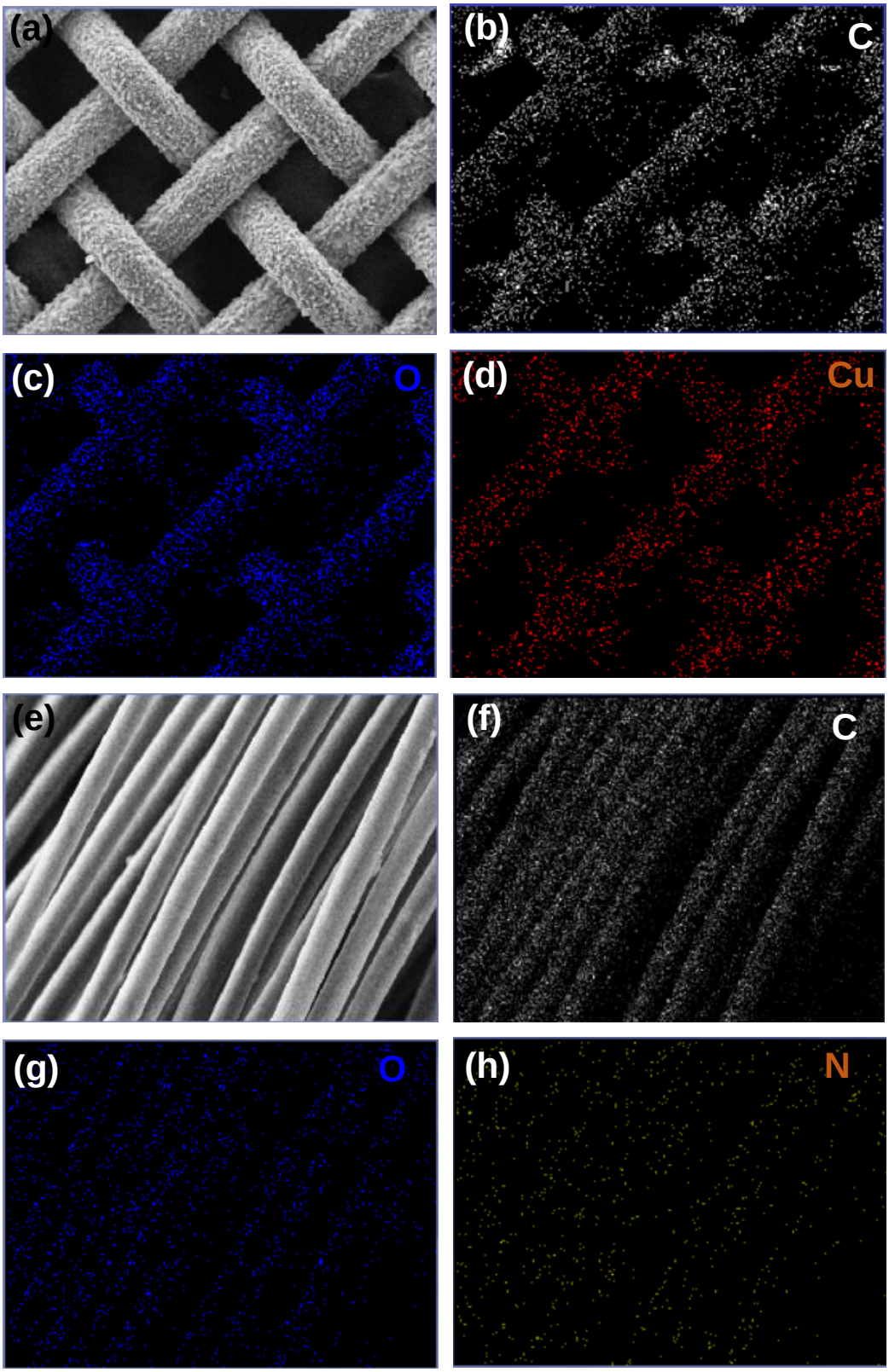

Fig. 3 Elemental mapping analysis: (a) Image of the selected area, (b) carbon, (c) oxygen and (d) nitrogen of HKUST-1 mesh; (e) image of the selected area, (f) carbon, (g) oxygen and (h) nitrogen of TEMPO@CC.

Fig. 2(f), and no huge differences between the pristine CC and TEMPO@CC were observed. Closer views of TEMPO@CC (Fig. 2(g),(h)) confirmed that fibrous configuration of carbon fibers in CC was well-retained and no obvious damage or destruction was noted. Nevertheless, Fig. 2(i) reveals that elements of N and O were detected, suggesting that CC had been modified and functionalized. Fig. 3(e)-(h) also display that elements of O and N were homogeneously distributed all over these fibers, suggesting that the surficial modification and functionalization on carbon fibers was uniformly-implemented.

Moreover, IR spectra of CC and TEMPO@CC were displayed in Fig. 4(b). While CC exhibited relatively limited IR peaks, TEMPO@CC showed several noticeable peaks in the range of 1000~1700 cm^{-1} and 2800~3000 cm^{-1}. In comparison to the IR spectrum of OH-TEMPO, these noticeable peaks of TEMPO@CC could be attributed to TEMPO. Specifically, the peaks at 875, 1580, 1620 cm^{-1} would be ascribed to C-H bonds derived from tetramethyl groups of TEMPO [46]. Additionally, the peak at 2944 cm^{-1} could be assigned to CH_3 bonds in TEMPO [46]. The presence of these peaks suggested that TEMPO was grafted onto CC. More importantly, as TEMPO is a strong radical, ESR analysis was then employed to determine TEMPO@CC (Fig. 4(c)). Even though no signal was observed in the case of CC, a typical three-line pattern with equal intensities [47, 48], which was attributed to TEMPO radicals [47, 48], could be easily measured. These characterizations all indicated that TEMPO was grafted onto CC.

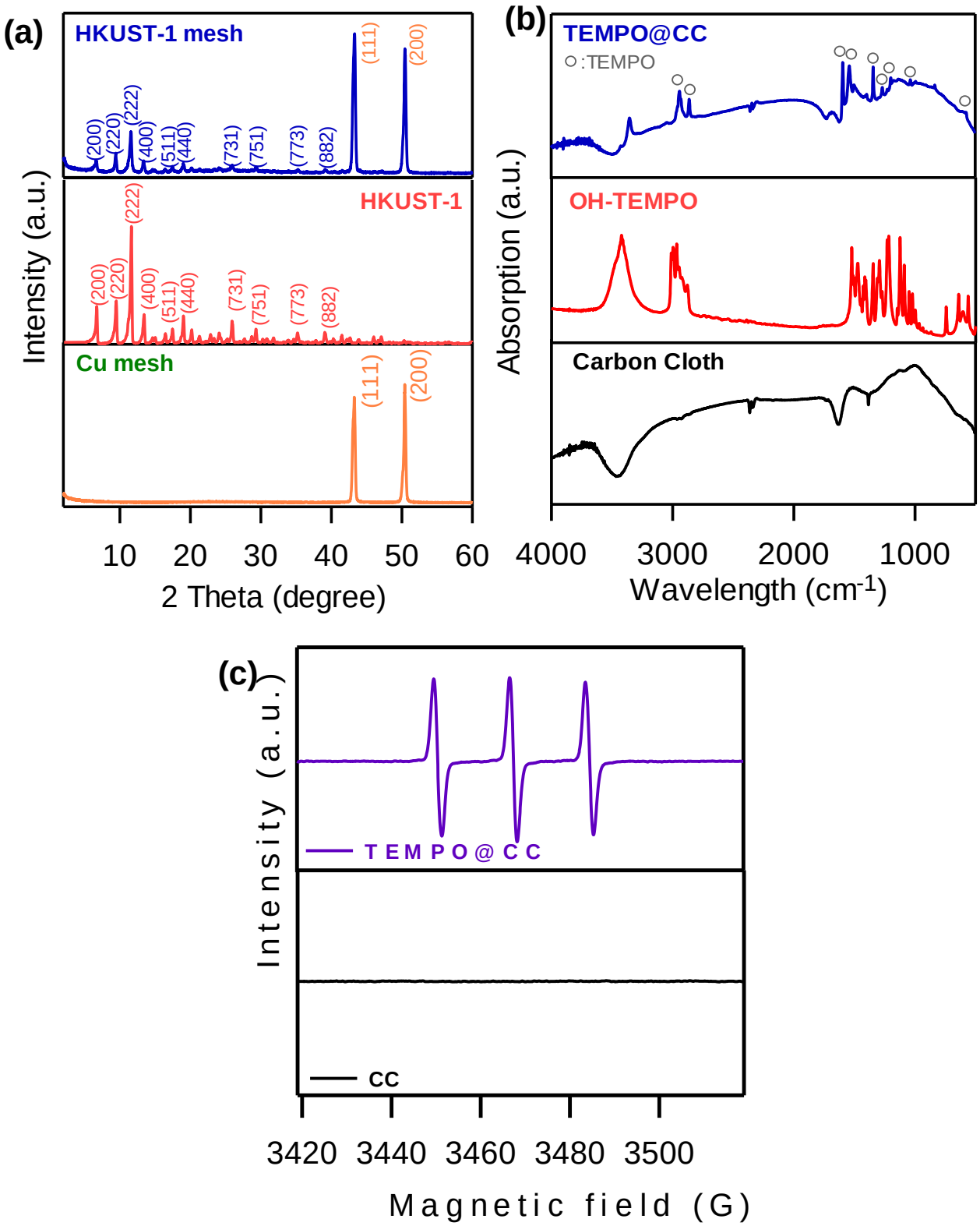

Fig. 4 (a) XRD patterns of HKUST-1 mesh, HKUST-1, and Cu mesh, (b) IR spectra of TEMPO@CC, CC, and TEMPO; and (c) ESR analyses of TEMPO@CC and CC.

As the Cu mesh and CC had been modified and deposited with HKUST-1 and TEMPO moieties, respectively, their textural properties might be also changed. Thus, their N_2 sorption isotherms were then measured. Fig. 5(a) shows N_2 sorption isotherms of pristine Cu mesh and HKUST-1 mesh. Since the pristine Cu mesh exhibited very smooth surface, its N_2 sorption capacity was extremely low, leading to a very low surface area of 10 m^2/g.

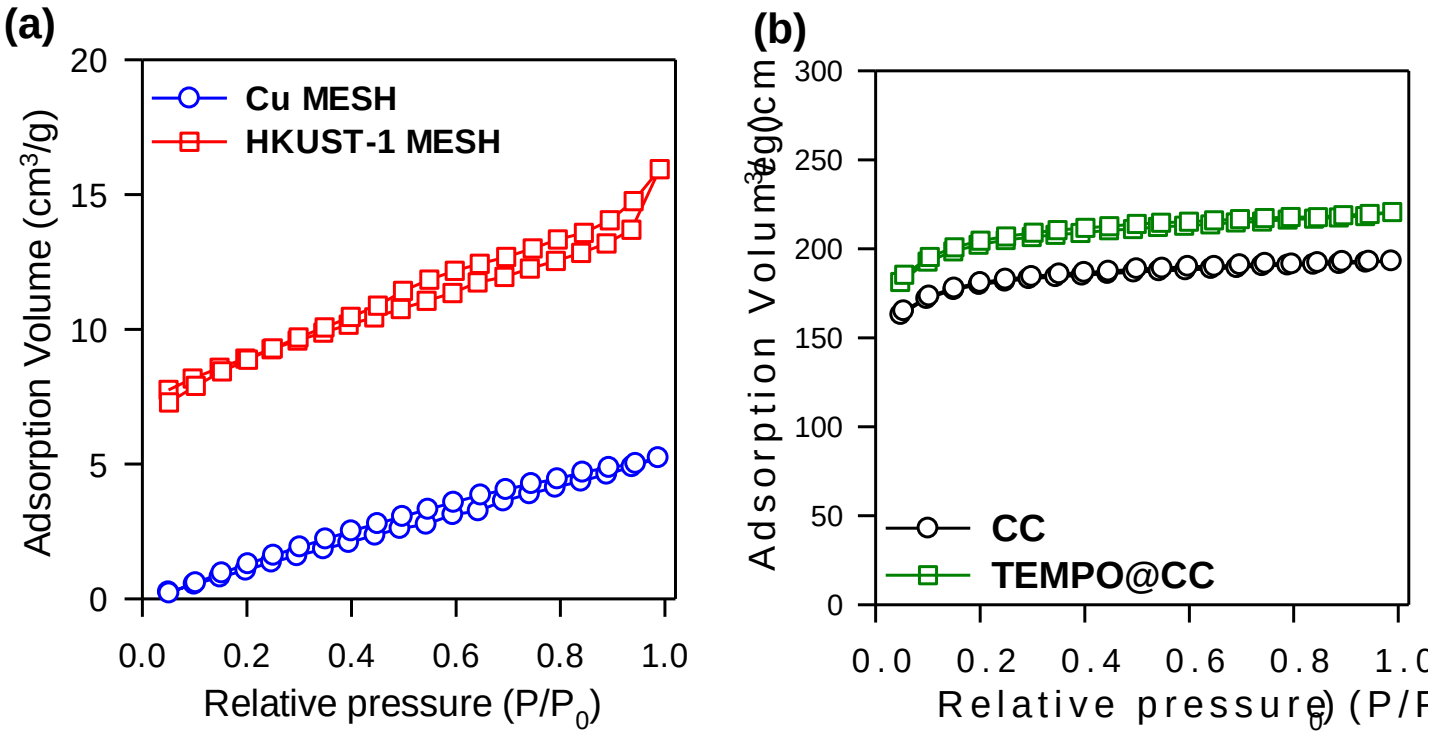

Fig. 5 N_2 sorption isotherms of (a) Cu mesh and HKUST-1 mesh; and (b) TEMPO@CC and CC.

Nevertheless, after growing HKUST-1 on the Cu mesh, HKUST-1 mesh certainly showed a much higher N^2 sorption and a small hysteresis loop could be also observed, validating that the formation of HKUST-1 enabled Cu mesh to show higher surface area (i.e., 30 m^2/g). On the other hand, N_2 sorption isotherms of pristine CC and TEMPO@CC could be seen in Fig. 5(b), and these two materials exhibited very similar isotherms as the fibrous structure of CC remained after the modifications. Nonetheless,

a slightly higher N_2 sorption was obtained by TEMPO@CC possibly because the acidic pretreatment (by HCl) might roughen the surface of carbon fibers, leading to a slightly higher surface area of 626.8 m^2/g than that of pristine CC (i.e., 558.4 m^2/g).

3.2 Conversion of VAL to VN by the sandwich-like catalytic system

As mentioned in the earlier section, VAL conversion using SCS was implemented by bundling HKUST-1 meshes and TEMPO@CC to form the SCS as displayed in Fig. 6(a), which was hanged by a Cu wire in the center of the reactor as demonstrated in Fig. 6(b). The reactants would then flow through and continuously contact with HKUST-1 meshes and TEMPO@CC as illustrated in Fig. 6(c).

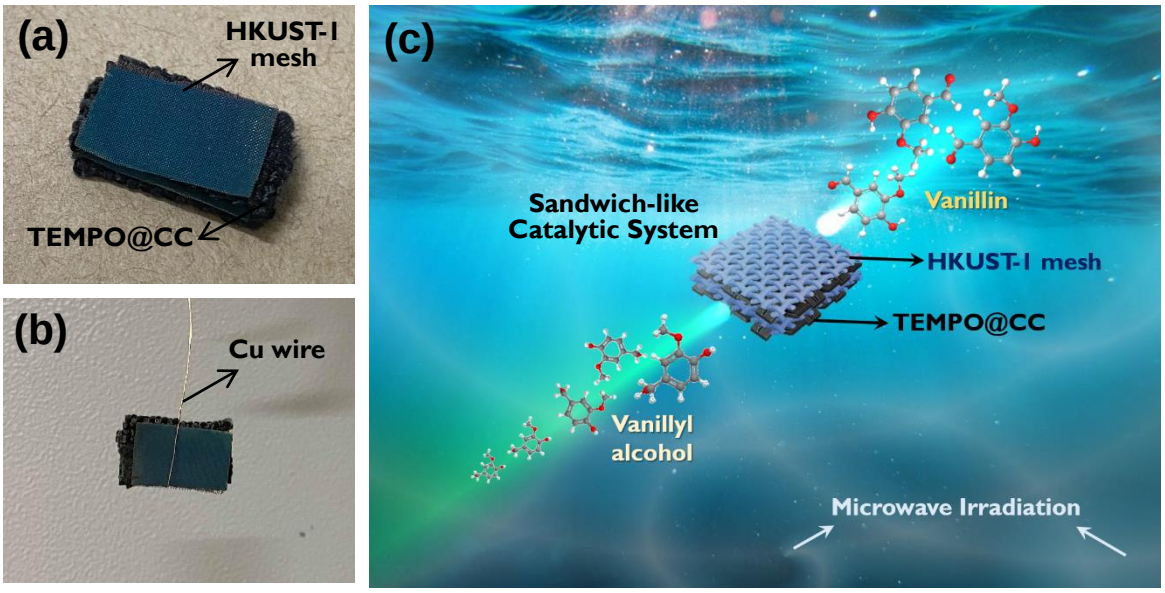

Fig. 6. (a) picture of the sandwich-like catalytic system consisting of inter-stacked HKUST-1 meshes and TEMPO@CC; (b) the sandwich-like catalytic system bundled and hanged by a Cu wire; and (c) illustration of flow-through reaction of VAL converted to VN via the sandwich-like catalytic system under microwave irradiation.

As VAL conversion to VN is a thermo-chemical reaction, heating processes are highly critical. Especially, since SCS consisted of the inter-stacked multilayers of active components, it is important to enable the SCS to achieve desired temperatures. Thus, in

the present study, two distinct heating methods were employed and compared: conventional heating by oven and MWI. Fig. 7(a) firstly shows VAL conversion by HKUST-1 meshes, TEMPO@CC and SCS (HKUST-1 meshes inter-stacked with TEMPO@CC) with COH. When HKUST-1 mesh alone was present, almost no VAL was converted and no VN could be detected.

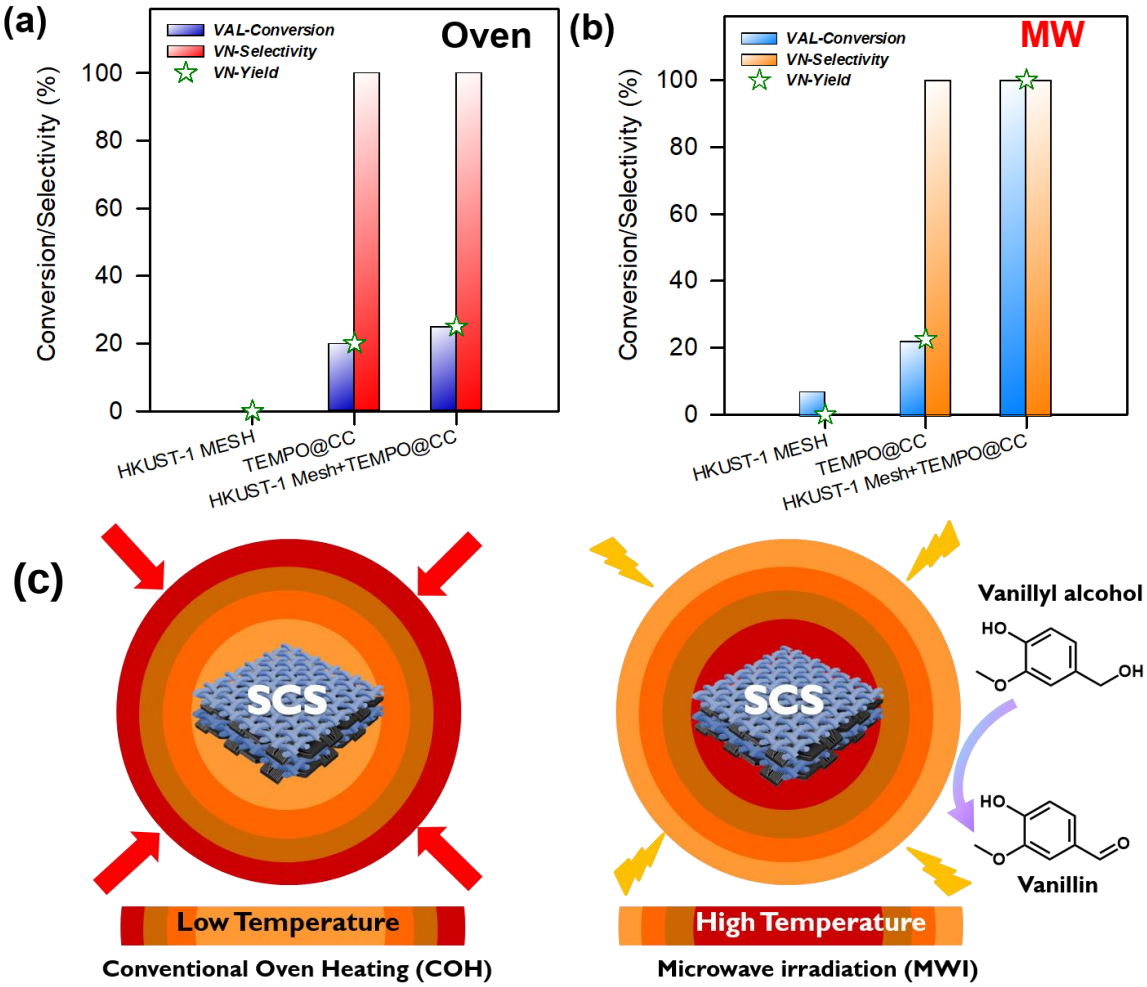

Figure 7. Conversion of VAL to VN using different materials (a) in a conventional oven and (b) under microwave irradiation (VAL = 10mg, IPA = 20 mL, SCS = 0.4 g).

On the other hand, when TEMPO@CC alone was then tested and it was slightly active and capable of a small fraction of VAL (C_{VAL} = 20%) with a very high selectivity for VN. Once TEMPO@CC was combined with HKUST-1 mesh, forming the SCS, C_{VAL} was slightly increased from 20 to 25% and the selectivity still remained very high.

These results demonstrated that TEMPO@CC itself had been active for oxidizing VAL to VN and the SCS could further enhance conversion slightly.

When the heating method was switched to microwave irradiation, HKUST-1 mesh alone seemed still ineffective to convert VAL to VN (Fig. 7(b)). On the other hand, VAL was also successfully converted to VN by TEMPO@CC under MWI and C_{VAL} seemed to increase slightly with MWI. Nevertheless, TEMPO@CC was still insufficient to achieve efficient conversion of VAL. However, once both HKUST-1 mesh and TEMPO@CC were inter-stacked to form SCS under MWI, its corresponding VAL conversion achieved 100% with S_{VN} = 100%, leading to Y_{VN} = 100%. This indicates that SCS was certainly capable of converting VAL to VN with high selectivity and yield, and MWI was powerful to enhance conversion of VAL.

The aforementioned comparison clearly indicates that that the heating method played a critical role for solvothermal reaction of VAL oxidation and MWI was certainly more advantageous than COH as MWI provided a more efficient heating process for rapid and intense heat from the interior of catalyst [49-52]. In particular, as MWI was adopted, the Cu-O group of HKUST-1 could absorb MW and obtain heat much more quickly from the interior of HKUST-1 [53], enabling it much more effective for VAL conversion. More importantly, since Cu-O groups of HKUST-1 were coordinated with the ligand, BTC, BTC would also absorb MWI and promote catalytic activities of Cu-O groups [53]. On the other hand, CC has been also validated as a strong MW absorber and CC should receive heat from the interior much quickly under MWI in contrast to conventional oven heating [54, 55].

Therefore, the enhancement of VAL conversion to VN by SCS under MWI could be ascribed to the feature that the Cu-O group of HKUST-1 and CC were more catalytic active because of fast and intense heat from the core center of catalysts [49, 50]. In

contrast, COH provided the highest temperature on the reactor wall but much lower temperature in the central region [49], resulting in much less effective conversion of VAL as illustrated in Fig. 7(c).

3.3 Effects of reaction temperature and time on VAL conversion by SCS

As VAL conversion to VN is a solvothermal reaction, reaction temperature was extremely critical for VAL oxidation and it would be also useful to investigate VAL conversion at relatively short durations under MWI. Fig. 8(a) displays VAL conversion efficiency as a function of temperature ranging from 60 to 120 °C.

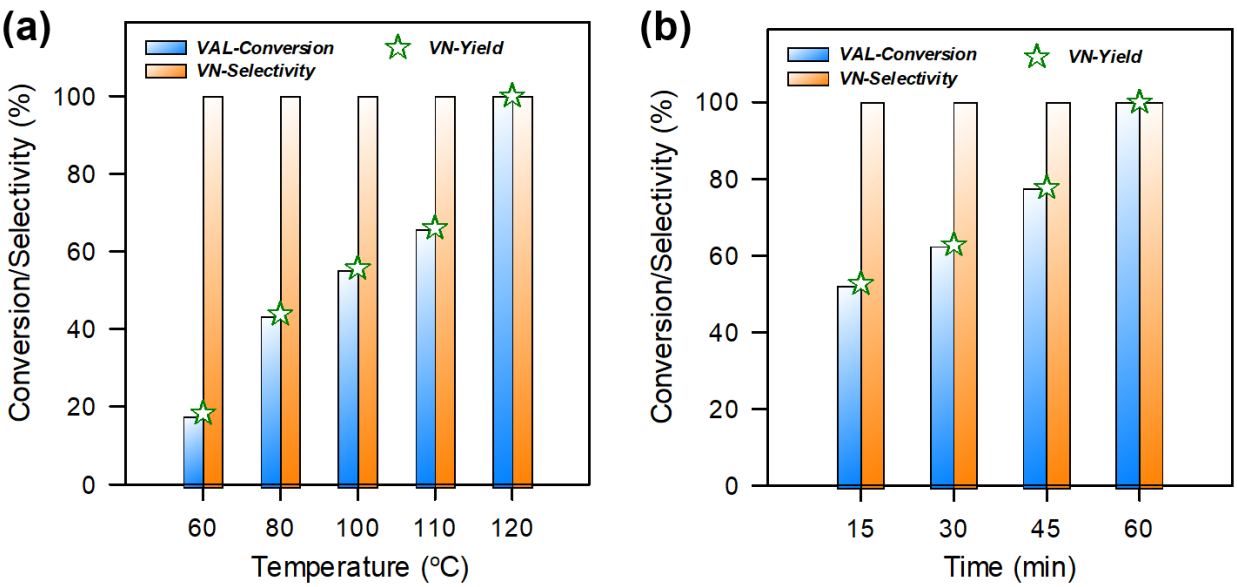

Fig. 8. Effects of (a) temperature (t = 60 min) and (b) time (T = 120 °C) on conversion efficiency of VAL to VN (VAL = 10mg, IPA = 20 mL, SCS = 0.4 g)

When the reaction temperature was low as 60 °C, VAL could be still oxidized to VN with C_{VAL} = 19%. Even though the conversion was relatively low, its corresponding selectivity was still 100%. Once the temperature further increased to 80 °C, C_{VAL} could be then raised to 43% while maintaining S_{VN} = 100%. At higher temperatures of 100,

110 and 120 °C, C_{VAL} further increased to 55, 66 and 100%, respectively, and S_{VN} remained consistent as 100%. This demonstrates that VAL could be also oxidized selectively to VN even at relatively low temperatures. Nevertheless, this result also suggests that temperature was validated as a crucial factor and 120 °C would be an optimal temperature for complete conversion of VAL to VN. Thus, 120 °C was then selected for further investigating effect of reaction duration.

Fig. 8(b) shows VAL conversion efficiency as a function of reaction time ranging from 15 to 60 min. As short as 15 min at 120 °C under MWI, C_{VAL} could reach 53% and S_{VN} was 100%. This signifies that a reaction duration of 15 min under MWI had been capable of converting more than a half of VAL to VN. As the reaction time further increased to 30 and 45 min, C_{VAL} was raised to 63 and 78%, respectively, revealing that a longer reaction time certainly enhanced VAL conversion while S_{VN} remained 100%. Once the reaction duration was extended to 60 min, C_{VAL} could reach 100% and, more importantly, no over-oxidation was observed as no vanillic acid was detected, demonstrating that SCS was highly advantageous and promising for VAL conversion. These results suggest that the optimal condition for VAL conversion by SCS is 120 °C for 60 min under MWI.

To further evaluate competitiveness of SCS for VAL conversion, Table 1 lists VAL conversion efficiencies of reported processes. One can notice that most of reported processes exhibited much lower conversions (ranging from 7 to 96%), and corresponding selectivities (ranging from 5 to 96.5%) and yields (ranging from 1.4 to 92.6%) were also relatively low in comparison to those obtained by SCS. This validates that SCS is certainly more useful than almost all reported systems.

Table 1. VAL to VN catalyzed by using various oxidation techniques.

Catalyst	***Oxidant***	***Temp.(°C)***	***VAL Con. (%)***	***VN Sel.(%)***	***VN Yield(%)***	***Ref.***
SCS	**air**	**120**	**100**	**100**	**100**	**This study**
Cu/TEMPO	air	90	99	93	91	[42]
TEMPO@SiO_2/Cu+	air	30	96	96.5	92.6	[27]
CuO/$MgAl_2O_4$	H_2O_2	90	67	74		[56]
CuO/$MgFe_2O_4$			53	46		
MnFe	O_2	100	21	79	21	[57]
FeFe			70	91	31	
CoFe			70	84	5	
NiFe			76	11	5	
CuFe			86	35	5	
ZnFe			46	19	15	
Au-Pd	air	RT	52.8	49.6	26.2	[58]
N-RGO/Mn_3O_4	air	120	26.4	19.2	5.1	[59]
nCo-MO	air	120	7.0	5.7	0.4	[60]
Co_3O_4	air	120	47.9	60.6	29	[26]
$MnCl_2$	H_2O_2	75	38	19	7.2	[6]
	H_2O_2	75	28	5	1.4	
	H_2O_2	80	89.6	49.4	44.3	
$CrCl_3$	H_2O_2	80	94.2	60.6	57.1	
$CoCl_2$	H_2O_2	80	48.1	33.9	16.3	

3.3 Potential mechanism of VAL conversion by SCS

As SCS was validated to successfully and effectively convert VAL to VN (Fig. 9(a)), it would be interesting to speculate the corresponding conversion mechanism. As SCS was comprised of the inter-stacked HKUST-1 mesh and TEMPO@CC, the Cu-O group of HKUST-1 would firstly react with VAL as illustrated in Fig. 9(b) [61, 62]. Subsequently, TEMPO@CC would then react with the intermediate of VAL to pull out a proton [61, 62], resulting in TEMPOH@CC and the product, VN. The resultant

TEMPOH would be then transformed back to TEMPO via mediation by O_2 [30, 40]. Through these catalytic reactions involving with the Cu-O group, TEMPO and VAL, VAL would be constantly and selectively converted to VAL [63].

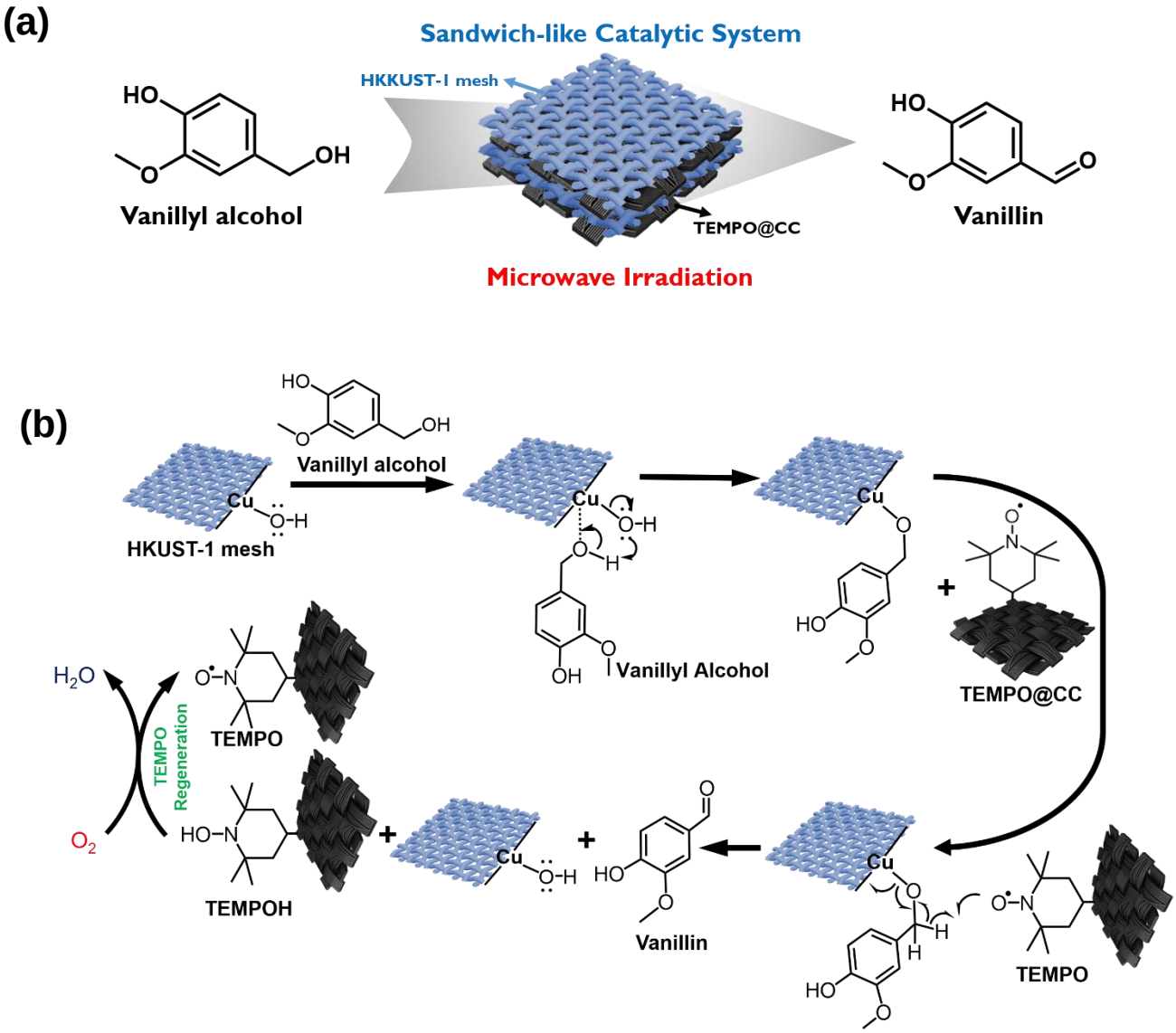

Fig. 9. (a) Illustration of VAL conversion to VN using the sandwich-like catalyst system (SCS), and (b) a proposed mechanism for VAL conversion to VN using the sandwich-like catalyst system (SCS).

3.4 Recyclability of SCS for VAL conversion

As SCS was proposed as a heterogeneous catalytic system, its recyclability would be critical and thus evaluated for multi-cyclic experiments of VAL oxidation. Fig. 10

shows continuous VAL conversion by SCS over 5 cycles and C_{VAL}, S_{VN} and Y_{VN} were remained almost the same (~100%) over the 5 cycles. This demonstrated that the catalytic activities of SCS, which consisted of HKUST-1 mesh and TEMPO@CC, were well retained and remained highly active for VAL conversion, indicating that SCS was stable, efficient and reusable for VAL oxidation to VN.

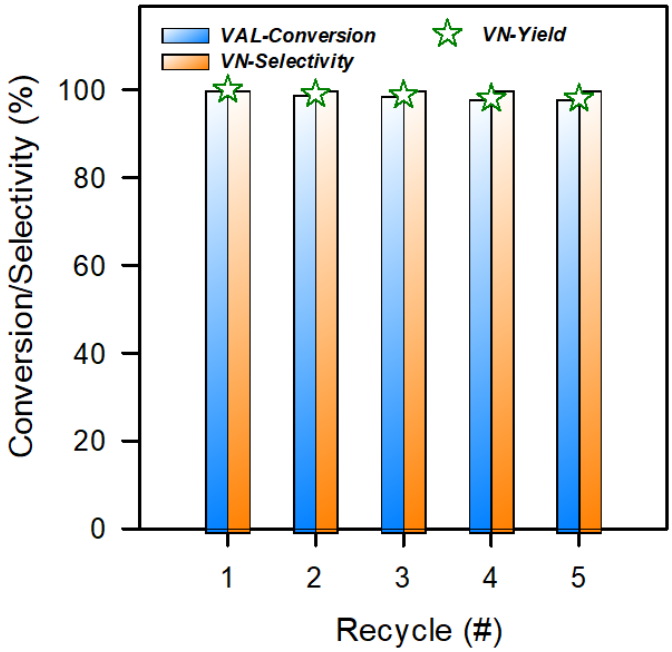

Figure 10. Recyclability of SCS for oxidation of VAL (VAL = 10mg, IPA = 20 mL, SCS = 0.4 g).

The used HKUST-1 mesh and TEMPO@CC can be also seen in Fig. 11(a) and (b), respectively. Their appearances suggested that HKUST-1 crystals were still retained on the surface of Cu mesh and the surface of used carbon fiber was almost unchanged. Furthermore, the XRD pattern of used HKUST-1 mesh (Fig. 11 (c)) was consistent to the theoretical XRD pattern of HKUST-1, indicating that crystalline structures of HKUST-1 remained. On the other hand, ESR analysis was adopted to examine whether TEMPO was retained in TEMPO. Fig. 11 (d) shows that the three-line hyperfine

splitting pattern (attributed to TEMPO) was still detected, validating that TEMPO moieties were preserved in the used TEMPO@CC. These results both demonstrated that SCS was highly stable and reusable for VAL conversion.

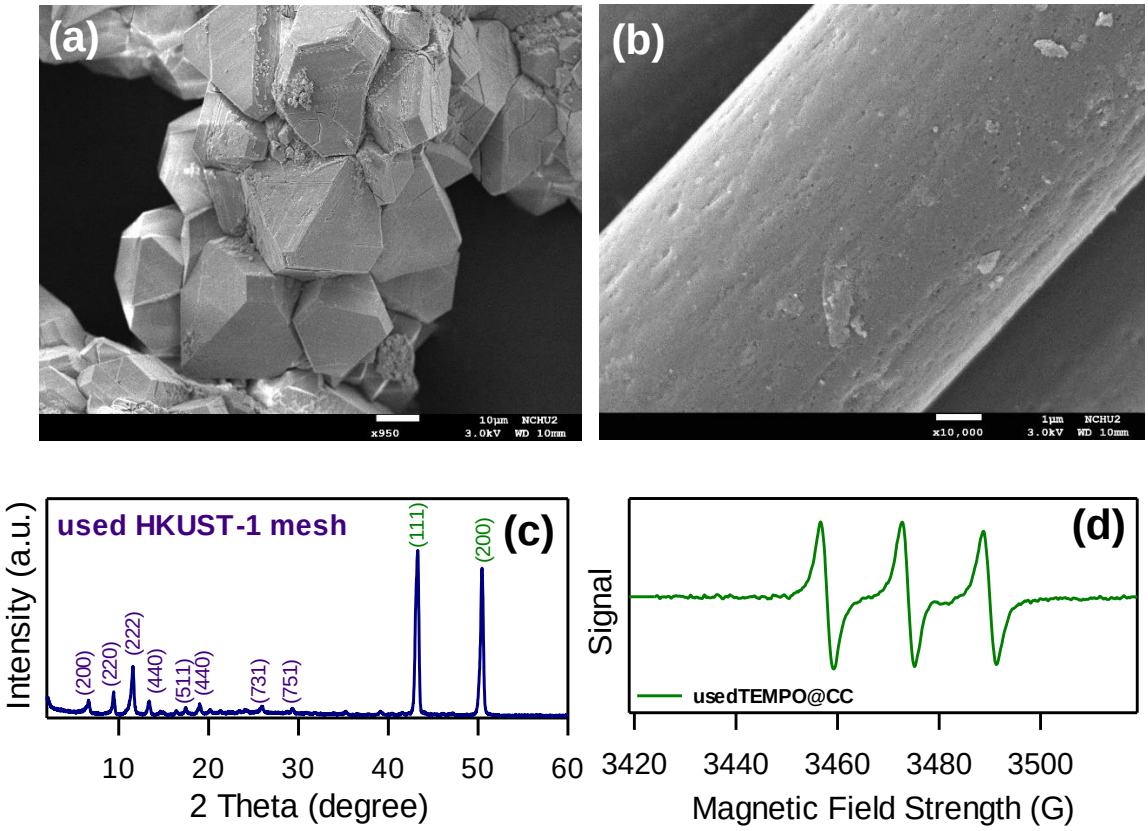

Fig. 11. SEM images of (a) HKUST-1 mesh and (b) TEMPO@CC; (c) XRD pattern of used HKUST-1 mesh and (d) ESR analysis of used TEMPO@CC.

4. Conclusions

In this study, a unique sandwich-like catalytic system (SCS) comprised of HKUST-1 mesh and TEMPO@CC was developed and fabricated as an integrated heterogeneous catalyst for VAL oxidation. Through the electro-chemical technique, Cu mesh was adopted as a source of Cu to grow HKUST-1 directly, whereas CC was functionalized by TEMPO via covalent bonds. These resultant sheet-like materials were then inter-stacked to allow layer-by-layer contacts between HKUST-1 and TEMPO, and flow-thru

reactions of VAL oxidation. Especially, such a SCS exhibited much higher conversion of VAL to VN under MWI than conventional oven heating. SCS was also capable of converting VAL to VN even at relatively low temperature as 60 °C for a very short duration of 15 min. As temperature and reaction time increased, SCS could achieve 100% of conversion, 100% of selectivity and 100% of yield of VN at 120 °C for 60 min. This full conversion of VAL to VN surpassed almost all the reported values by other processes in literature, validating its promising advantages. In addition, SCS could be also reusable and continuously implemented for VAL conversion to VN. The used HKUST-1 mesh could retain crystalline structures of HKUST-1, whereas TEMPO was also preserved on TEMPO@CC, indicating that SCS would be a stable and reusable integrated catalyst for VAL oxidation to VN.

Acknowledgement:

This work is supported by the Ministry of Science and Technology (MOST)(109-2636-E-005-003-), Taiwan, and financially supported by the "Innovation and Development Center of Sustainable Agriculture" from The Featured Areas Research Center Program within the framework of the Higher Education Sprout Project by the Ministry of Education (MOE), Taiwan.

References:

[1] R.D. Perlack, L.L. Wright, A.F. Turhollow, R.L. Graham, B.J. Stokes, D.C. Erbach, Biomass as feedstock for a bioenergy and bioproducts industry: the technical feasibility of a billion-ton annual supply, in: DTIC Document, 2005.

[2] R. Behling, S. Valange, G. Chatel, Heterogeneous catalytic oxidation for lignin valorization into valuable chemicals: what results? What limitations? What trends?, Green Chemistry, 18 (2016) 1839-1854.

[3] H. Lange, S. Decina, C. Crestini, Oxidative upgrade of lignin – Recent routes

reviewed, European Polymer Journal, 49 (2013) 1151-1173.

[4] A. Azarpira, J. Ralph, F. Lu, Catalytic Alkaline Oxidation of Lignin and its Model Compounds: a Pathway to Aromatic Biochemicals, BioEnergy Research, 7 (2014) 78-86.

[5] J. Dai, A.F. Patti, K. Saito, Recent developments in chemical degradation of lignin: catalytic oxidation and ionic liquids, Tetrahedron Letters, 57 (2016) 4945-4951.

[6] J. Pan, J. Fu, X. Lu, Microwave-Assisted Oxidative Degradation of Lignin Model Compounds with Metal Salts, Energy & Fuels, 29 (2015) 4503-4509.

[7] L. Cao, I.K.M. Yu, Y. Liu, X. Ruan, D.C.W. Tsang, A.J. Hunt, Y.S. Ok, H. Song, S. Zhang, Lignin valorization for the production of renewable chemicals: State-of-the-art review and future prospects, Bioresour Technol, 269 (2018) 465-475.

[8] M. Culebras, H. Geaney, A. Beaucamp, P. Upadhyaya, E. Dalton, K.M. Ryan, M.N. Collins, Bio-derived Carbon Nanofibres from Lignin as High-Performance Li-Ion Anode Materials, ChemSusChem, 12 (2019) 4516-4521.

[9] W.J. Liu, H. Jiang, H.Q. Yu, Thermochemical conversion of lignin to functional materials: a review and future directions, Green Chemistry, 17 (2015) 4888-4907.

[10] S. Gharehkhani, Y. Zhang, P. Fatehi, Lignin-derived platform molecules through TEMPO catalytic oxidation strategies, Progress in Energy and Combustion Science, 72 (2019) 59-89.

[11] A. Jha, C.V. Rode, Highly selective liquid-phase aerobic oxidation of vanillyl alcohol to vanillin on cobalt oxide (Co3O4) nanoparticles, New Journal of Chemistry, 37 (2013) 2669-2674.

[12] S. Saha, S.B.A. Hamid, T.H. Ali, Catalytic evaluation on liquid phase oxidation of vanillyl alcohol using air and H2O2 over mesoporous Cu-Ti composite oxide, Applied Surface Science, 394 (2017) 205-218.

[13] A. Jha, D. Mhamane, A. Suryawanshi, S.M. Joshi, P. Shaikh, N. Biradar, S. Ogale, C.V. Rode, Triple nanocomposites of CoMn2O4, Co3O4 and reduced graphene oxide for oxidation of aromatic alcohols, Catalysis Science & Technology, 4 (2014) 1771-1778.

[14] Z. Yuan, S. Chen, B. Liu, Nitrogen-doped reduced graphene oxide-supported Mn3O4: An efficient heterogeneous catalyst for the oxidation of vanillyl alcohol to vanillin, Journal of Materials Science, 52 (2017) 164-172.

[15] S. Ramana, B.G. Rao, P. Venkataswamy, A. Rangaswamy, B.M. Reddy, Nanostructured Mn-doped ceria solid solutions for efficient oxidation of vanillyl alcohol, Journal of Molecular Catalysis A: Chemical, 415 (2016) 113-121.

[16] M. Fache, B. Boutevin, S. Caillol, Vanillin Production from Lignin and Its Use as a Renewable Chemical, ACS Sustainable Chemistry & Engineering, 4 (2016) 35-46.

[17] J.-Y. Lin, H.-K. Lai, K.-Y.A. Lin, Rapid microwave-hydrothermal conversion of lignin model compounds to value-added products via catalytic oxidation using metal organic frameworks, Chemical Papers, (2018).

[18] K.-Y.A. Lin, H.-K. Lai, Z.-Y. Chen, Selective generation of vanillin from catalytic oxidation of a lignin model compound using ZIF-derived carbon-supported cobalt nanocomposite, J Taiwan Inst Chem Eng, (2017).

[19] J. Pan, J. Fu, S. Deng, X. Lu, Microwave-Assisted Degradation of Lignin Model Compounds in Imidazolium-Based Ionic Liquids, Energy & Fuels, 28 (2014) 1380-1386.

[20] J.A.G.d. Silveira, É.M.L. Rabelo, P.C.S. Lima, B.N. Chaves, M.F.B. Ribeiro, Post-mortem hemoparasite detection in free-living Brazilian brown brocket deer (Mazama gouazoubira, Fischer 1814), Revista Brasileira de Parasitologia Veterinária, 23 (2014) 206-215.

[21] R. Yepez, S. Garcia, P. Schachat, M. Sanchez-Sanchez, J.H. Gonzalez-Estefan, E. Gonzalez-Zamora, I.A. Ibarra, J. Aguilar-Pliego, Catalytic activity of HKUST-1 in the oxidation of trans-ferulic acid to vanillin, New Journal of Chemistry, 39 (2015) 5112-5115.

[22] E. Sánchez-González, A. López-Olvera, O. Monroy, J. Aguilar-Pliego, J. Gabriel Flores, A. Islas-Jácome, M.A. Rincón-Guevara, E. González-Zamora, B. Rodríguez-Molina, I.A. Ibarra, Synthesis of vanillin via a catalytically active Cu(ii)-metal organic polyhedron, CrystEngComm, 19 (2017) 4142-4146.

[23] P. Elamathi, M.K. Kolli, G. Chandrasekar, Catalytic Oxidation of Vanillyl Alcohol Using FeMCM-41 Nanoporous Tubular Reactor, International Journal of Nanoscience, 17 (2017).

[24] R. Yepez, J.F. Illescas, P. Gijon, M. Sanchez-Sanchez, E. Gonzalez-Zamora, R. Santillan, J.R. Alvarez, I.A. Ibarra, J. Aguilar-Pliego, HKUST-1 as a Heterogeneous Catalyst for the Synthesis of Vanillin, J Vis Exp, (2016).

[25] J.G. Flores, E. Sánchez-González, A. Gutiérrez-Alejandre, J. Aguilar-Pliego, A. Martínez, T. Jurado-Vázquez, E. Lima, E. González-Zamora, M. Díaz-García, M. Sánchez-Sánchez, I.A. Ibarra, Greener synthesis of Cu-MOF-74 and its catalytic use for the generation of vanillin, Dalton Transactions, 47 (2018) 4639-4645.

[26] R. Behling, G. Chatel, S. Valange, Sonochemical oxidation of vanillyl alcohol to vanillin in the presence of a cobalt oxide catalyst under mild conditions, Ultrasonics Sonochemistry, 36 (2017) 27-35.

[27] M.-W. Zheng, K.-Y.A. Lin, C.-H. Lin, TEMPO-Functionalized Silica as an Efficient and Recyclable Oxidation Catalyst for Conversion of a Lignin Model Compound to Value-Added Products, Waste and Biomass Valorization, (2019).

[28] J.-Y. Lin, J. Lee, K.-Y.A. Lin, Microwave-Assisted Catalyst-Free Oxidative

Conversion of a Lignin Model Compound to Value-Added Products Using TEMPO, Waste and Biomass Valorization, (2019).

[29] A.J. Fatiadi, R. Schaffer, An Improved Procedure for Synthesis of DL-4-Hydroxy-3-methoxymandelic Acid (DL-"Vanillyl"-mandelic Acid, VMA), J Res Natl Bur Stand A Phys Chem, 78A (1974) 411-412.

[30] P.D. Sainsbury, E.M. Hardiman, M. Ahmad, H. Otani, N. Seghezzi, L.D. Eltis, T.D.H. Bugg, Breaking Down Lignin to High-Value Chemicals: The Conversion of Lignocellulose to Vanillin in a Gene Deletion Mutant of Rhodococcus jostii RHA1, ACS Chemical Biology, 8 (2013) 2151-2156.

[31] H.P. Chen, M. Chow, C.C. Liu, A. Lau, J. Liu, L.D. Eltis, Vanillin catabolism in Rhodococcus jostii RHA1, Applied and environmental microbiology, 78 (2012) 586-588.

[32] L. Yan, P. Chen, S. Zhang, S. Li, X. Yan, N. Wang, N. Liang, H. Li, Biotransformation of ferulic acid to vanillin in the packed bed-stirred fermentors, Scientific Reports, 6 (2016) 34644.

[33] A. Converti, B. Aliakbarian, J.M. Domínguez, G. Bustos Vázquez, P. Perego, Microbial production of biovanillin, Braz J Microbiol, 41 (2010) 519-530.

[34] Z. Yuan, B. Liu, P. Zhou, Z. Zhang, Q. Chi, Aerobic oxidation of biomass-derived 5-hydroxymethylfurfural to 2,5-diformylfuran with cesium-doped manganese dioxide, Catalysis Science & Technology, 8 (2018) 4430-4439.

[35] K.-Y.A. Lin, H.-K. Lai, Z.-Y. Chen, Selective generation of vanillin from catalytic oxidation of a lignin model compound using ZIF-derived carbon-supported cobalt nanocomposite, Journal of the Taiwan Institute of Chemical Engineers, 78 (2017) 337-343.

[36] H.-K. Lai, Y.-Z. Chou, M.-H. Lee, K.-Y.A. Lin, Coordination polymer-derived cobalt nanoparticle-embedded carbon nanocomposite as a magnetic multi-functional catalyst for energy generation and biomass conversion, Chemical Engineering Journal, 332 (2018) 717-726.

[37] S. Saha, S.B. Abd Hamid, Nanosized spinel Cu-Mn mixed oxide catalyst prepared via solvent evaporation for liquid phase oxidation of vanillyl alcohol using air and H2O2, RSC Adv, 6 (2016) 96314-96326.

[38] M. Shilpy, M.A. Ehsan, T.H. Ali, S.B. Abd Hamid, M.E. Ali, Performance of cobalt titanate towards H2O2 based catalytic oxidation of lignin model compound, RSC Adv, 5 (2015) 79644-79653.

[39] J.M. Hoover, S.S. Stahl, Highly Practical Copper(I)/TEMPO Catalyst System for Chemoselective Aerobic Oxidation of Primary Alcohols, J Am Chem Soc, 133 (2011) 16901-16910.

[40] N.J. Hill, J.M. Hoover, S.S. Stahl, Aerobic Alcohol Oxidation Using a

Copper(I)/TEMPO Catalyst System: A Green, Catalytic Oxidation Reaction for the Undergraduate Organic Chemistry Laboratory, Journal of Chemical Education, 90 (2013) 102-105.

[41] J.M. Hoover, B.L. Ryland, S.S. Stahl, Mechanism of Copper(I)/TEMPO-Catalyzed Aerobic Alcohol Oxidation, J Am Chem Soc, 135 (2013) 2357-2367.

[42] J.-Y. Lin, K.-Y.A. Lin, Catalytic conversion of a lignin model compound to value-added products using Cu/TEMPO-catalyzed aerobic oxidation, Biomass Conversion and Biorefinery, 9 (2019) 617-623.

[43] S. Barna, E. Ott, T. Nguyen, M. Shannon, A. Scheeline, Silica Adsorbents and Peroxide Functionality for Removing Paraquat from Wastewater, Journal of Environmental Engineering, 139 (2013) 975-985.

[44] B.L. Ryland, S.S. Stahl, Practical Aerobic Oxidations of Alcohols and Amines with Homogeneous Copper/TEMPO and Related Catalyst Systems, Angewandte Chemie International Edition, 53 (2014) 8824-8838.

[45] T.S. Hansen, I. Sádaba, E.J. García-Suárez, A. Riisager, Cu catalyzed oxidation of 5-hydroxymethylfurfural to 2,5-diformylfuran and 2,5-furandicarboxylic acid under benign reaction conditions, Applied Catalysis A: General, 456 (2013) 44-50.

[46] D.L. Pavia, G.M. Lampman, G.S. Kriz, J.A. Vyvyan, Introduction to Spectroscopy, Cengage Learning, 2008.

[47] R. Luo, M. Li, C. Wang, M. Zhang, M.A. Nasir Khan, X. Sun, J. Shen, W. Han, L. Wang, J. Li, Singlet oxygen-dominated non-radical oxidation process for efficient degradation of bisphenol A under high salinity condition, Water Research, 148 (2019) 416-424.

[48] K.C. Das, C.K. Das, Thioredoxin, a Singlet Oxygen Quencher and Hydroxyl Radical Scavenger: Redox Independent Functions, Biochemical and Biophysical Research Communications, 277 (2000) 443-447.

[49] Z.M.A. Bundhoo, Microwave-assisted conversion of biomass and waste materials to biofuels, Renewable and Sustainable Energy Reviews, 82 (2018) 1149-1177.

[50] P. Chen, Q. Xie, Z. Du, F.C. Borges, P. Peng, Y. Cheng, Y. Wan, X. Lin, Y. Liu, R. Ruan, Microwave-Assisted Thermochemical Conversion of Biomass for Biofuel Production, in: Z. Fang, J.R.L. Smith, X. Qi (Eds.) Production of Biofuels and Chemicals with Microwave, Springer Netherlands, Dordrecht, 2015, pp. 83-98.

[51] Z. Zhang, Z.K. Zhao, Microwave-assisted conversion of lignocellulosic biomass into furans in ionic liquid, Bioresour Technol, 101 (2010) 1111-1114.

[52] C. Li, Z. Zhang, Z.K. Zhao, Direct conversion of glucose and cellulose to 5-hydroxymethylfurfural in ionic liquid under microwave irradiation, Tetrahedron Letters, 50 (2009) 5403-5405.

[53] T.-Y. Lin, K.-Y.A. Lin, Microwave-enhanced catalytic transfer hydrogenation of

levulinic acid to γ-valerolactone using zirconium-based metal organic frameworks: A comparative study with conventional heating processes, Journal of the Taiwan Institute of Chemical Engineers, 96 (2019) 321-328.

[54] N. Zhao, T. Zou, C. Shi, J. Li, W. Guo, Microwave absorbing properties of activated carbon-fiber felt screens (vertical-arranged carbon fibers)/epoxy resin composites, Materials Science and Engineering: B, 127 (2006) 207-211.

[55] W. Ye, W. Li, Q. Sun, J. Yu, Q. Gao, Microwave absorption properties of lightweight and flexible carbon fiber/magnetic particle composites, RSC Adv, 8 (2018) 24780-24786.

[56] B. Rahmanivahid, M. Pinilla-de Dios, M. Haghighi, R. Luque, Mechanochemical Synthesis of CuO/MgAl2O4 and MgFe2O4 Spinels for Vanillin Production from Isoeugenol and Vanillyl Alcohol, Molecules, 24 (2019).

[57] M.-W. Zheng, H.-K. Lai, K.-Y.A. Lin, Valorization of Vanillyl Alcohol by Pigments: Prussian Blue Analogue as a Highly-Effective Heterogeneous Catalyst for Aerobic Oxidation of Vanillyl Alcohol to Vanillin, Waste and Biomass Valorization, (2018) 1-10.

[58] M. Wu, J.-H. Pang, P.-P. Song, J.-J. Peng, F. Xu, Q. Li, X.-M. Zhang, Visible light-driven oxidation of vanillyl alcohol in air with Au–Pd bimetallic nanoparticles on phosphorylated hydrotalcite, New Journal of Chemistry, 43 (2019) 1964-1971.

[59] Z. Yuan, S. Chen, B. Liu, Nitrogen-doped reduced graphene oxide-supported Mn3O4: An efficient heterogeneous catalyst for the oxidation of vanillyl alcohol to vanillin, Journal of Materials Science, 52 (2016) 164-172.

[60] A. Jha, D. Mhamane, A. Suryawanshi, S.M. Joshi, P. Shaikh, N. Biradar, S. Ogale, C.V. Rode, Triple nanocomposites of CoMn2O4, Co3O4 and reduced graphene oxide for oxidation of aromatic alcohols, Catalysis Science & Technology, 4 (2014).

[61] A. Dhakshinamoorthy, M. Alvaro, H. Garcia, Aerobic Oxidation of Benzylic Alcohols Catalyzed by Metal−Organic Frameworks Assisted by TEMPO, ACS Catalysis, 1 (2010) 48-53.

[62] N.J. Hill, J.M. Hoover, S.S. Stahl, Aerobic Alcohol Oxidation Using a Copper(I)/TEMPO Catalyst System: A Green, Catalytic Oxidation Reaction for the Undergraduate Organic Chemistry Laboratory, Journal of Chemical Education, 90 (2012) 102-105.

[63] W.-C. Yun, T.-Y. Lin, H.-Y. Chiu, K.-Y.A. Lin, Microwave Irradiation-Enhanced Catalytic Transfer Hydrogenation of Levulinic Acid to γ-Valerolactone Using Ruthenium: A Comparative Study with Conventional Heating Processes, Waste and Biomass Valorization, (2019).

Declaration of interests

☒ The authors declare that they have no known competing financial interests or personal relationships that could have appeared to influence the work reported in this paper.

☐The authors declare the following financial interests/personal relationships which may be considered as potential competing interests: